https://doi.org/10.5194/egusphere-2022-970
Preprint. Discussion started: 11 October 2022

Southern outlet of the Northeast Greenland Ice Stream, NE Greenland: post-Last Glacial Maximum response to climate warming

Authors: Kevin Zoller[1]; Jan Sverre Laberg[1]; Tom Arne Rydningen[1], Katrine Husum[2] & Matthias Forwick[1]

[1]Department of Geosciences, UiT The Arctic University of Norway, Box 6050 Langnes, NO-9037 Tromsø, Norway [2]Norwegian Polar Institute, Box 6606 Langnes, NO-9296 Tromsø, Norway

Correspondence to: Kevin Zoller (kevin.zoller3@gmail.com)

Abstract

The Greenland Ice Sheet (GrIS) responds rapidly to the present climate, therefore, its response to the predicted future warming is of concern. To learn more about this, decoding its behavior during past periods of warmer than present climate is important. However, due to the scarcity of marine studies reconstructing ice sheet conditions on the Northeast Greenland shelf and adjacent fjords including the position of the ice sheet over marine regions, the timing of the deglaciation, and its connection to forcing factors including the Holocene Thermal Maximum (HTM) on NE Greenland remain poorly constrained. This paper aims to use bathymetric data and the analysis of sediment gravity cores to enhance our understanding of ice dynamics of the GrIS near the southern outlet of the Northeast Greenland Ice Stream (NGIS), as well as give insight into the timing of deglaciation and provide a palaeoenvironmental reconstruction of southwestern Dove Bugt and Bessel Fjord since the Last Glacial Maximum (LGM). The swath bathymetry data displayed in this study is the first time the bathymetry for Bessel Fjord has become available. North-south oriented glacial lineations, and the absence of pronounced moraines in southwest Dove Bugt, an inner continental shelf embayment (trough), suggests the southwards and offshore flow of the southern branch of the NGIS, Storstrømmen.
Sedimentological data suggests that an ice body, theorized to be the NGIS, may have retreated from the region slightly before ~11.2 ka BP (in the Preboreal period). The seabed morphology of Bessel Fjord, a fjord terminating in southern Dove Bugt, includes numerous basins, separated by thresholds. The position of basin thresholds, which include some recessional moraines, suggest that the GrIS had undergone multiple halts or readvances during deglaciation. A minimum age of 7.2 ka BP is proposed for the retreat of ice to or west of its present-day position in the Bessel Fjord catchment area. This suggests that the GrIS retreated from the marine realm in early Holocene, around the time of the onset of the Holocene Thermal Maximum in this region, a period when the mean July temperature according to Bennike et al., (2008) was at least 2-3 °C higher than at present, and remained at or west of this onshore position for the remainder of the Holocene. The transition from predominantly mud to muddy sand layers in a mid-fjord core at ~4 ka BP may be the result of increased sediment input from nearby and growing ice caps. This shift may suggest that in late Holocene (Meghalayan), a period characterized by a temperature drop to modern values, ice caps in Bessel Fjord fluctuated with greater sensitivity to climatic conditions than the NE sector of the GrIS.

https://doi.org/10.5194/egusphere-2022-970
Preprint. Discussion started: 11 October 2022

1. Introduction

Ice mass loss from the Greenland Ice Sheet (GrIS) has accelerated during the 21 century, making it the current largest individual contributor to sea level rise (King et al., 2020). This introduction of a substantial quantity of fresh water may have ramifications for global ocean circulations as well as the climate (Rahmstorf et al., 2015). Approximately 12% of the ice from the GrIS is transported to the coast through the Northeast Greenland Ice Stream (NGIS) (Larsen et al., 2018) and therefore has a substantial impact on the mass balance of the ice sheet and a potential to contribute to sea level rise. Currently, two of the three marine terminating outlet glaciers that are supplied by the NGIS are in retreat (Mouginot et al., 2015), where the southernmost branch, Storstrømmen in Dove Bugt (Figs. 1a & 1b), is currently in a building phase following a 1978-1984 surge (Khan et al., 2014; Reeh et al., 1994; Larsen et al., 2018). While there are numerous modern studies on the current state of the NGIS during the past decades to century, there is a scarcity of data concerning the position and dynamics of the ice stream, and other local Northeast Greenland outlet glaciers, on a multi-century to millennia scale over marine regions. Considering that the global mean temperature is expected to continue to rise (Stocker et al., 2013), and that the Arctic will experience an amplification effect (Cohen et al., 2014), looking to the past, especially during warmer than present periods (i.e. the Holocene Thermal Maximum (HTM)), may provide an important insight into the future behavior of the ice sheet.

Marine studies have found evidence for past advancement and retreat of the NGIS along the continental shelf offshore Northeast Greenland (Evans et al., 2009; Winkelmann et al., 2010; Arndt et al., 2015, 2017; Laberg et al., 2017; Arndt, 2018; Olsen et al., 2020). Geomorphological findings in Store Koldewey Trough, a major shelf trough northeast of the study area (Fig. 1b), suggests that the ice sheet may have reached the shelf break in this area during the LGM (Laberg et al., 2017; Olsen et al., 2020), but a concise understanding of the timing and dynamics of the ice sheet and ice stream over coastal and fjord regions during the subsequent deglaciation remains to be established. Terrestrial dating (e.g. cosmogenic nuclide dates and lake studies) has provided further insight into when terrestrial regions had become deglaciated, and how the climate has changed in these areas (e.g. Björck & Persson, 1981; Björck et al., 1994; Wagner et al., 2008; Klug, Schmidt, et al., 2009; Schmidt et al., 2011; Briner et al., 2016; Skov et al., 2020). However, a proper integration with marine data to establish a detailed chronology of the deglaciation is still pending.

Swath bathymetry and gravity cores data from southwestern Dove Bugt (i.e. Store Bælt) and Bessel Fjord (Fig. 1), presented for the first time in this study, has been used to further refine our understanding of how the GrIS and NGIS responded to changes in palaeoclimatic conditions from the LGM through the Holocene, including the HTM. Through this analysis we aim to reconstruct regional ice dynamics from both full-glacial conditions and during overall retreat and put our findings into the larger context of the dynamics of the Northeast Greenland Ice Sheet during these periods. Additionally, this study aims to refine our understanding about the timing of deglaciation over marine areas and compare findings to nearby terrestrial regions including the Store Koldewey island and Hochstetter Forland/Shannon Ø. Results will also contribute to our understanding of palaeoenvironmental conditions throughout the Holocene for the NE Greenland fjords and inner shelf areas.

https://doi.org/10.5194/egusphere-2022-970
Preprint. Discussion started: 11 October 2022

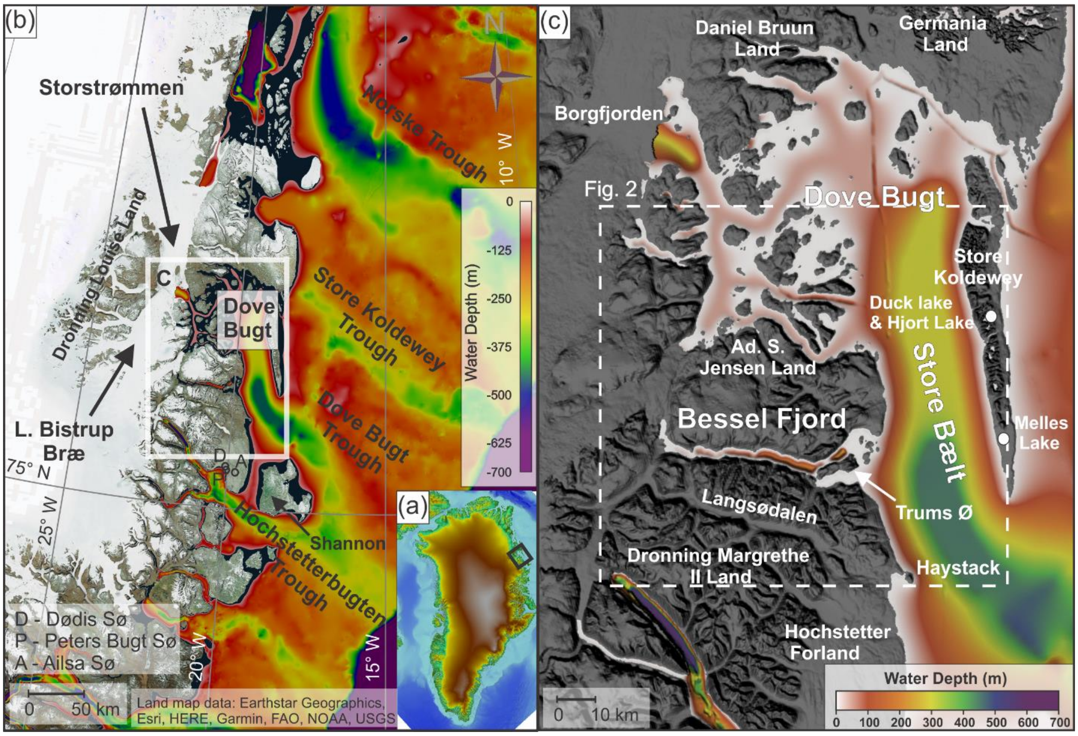

Figure 1. (a) An image of Greenland, using IBCAO 4.0 400x400m (Jakobsson et al., 2020)*, with a black box surrounding the study area. (b) Bathymetry of northern East Greenland displayed using IBCAO 4.0 200x200m data* (Jakobsson et al., 2020) *and land is displayed using a World Imagery satellite image (Earthstar Geographics | Esri) made available through GlobalMapper. The white box surrounds the position of Fig. 1c. (c) Bathymetry of Dove Bugt and Bessel Fjord and surrounding land areas displayed using the IBCAO 4.0 200x200m data* (Jakobsson et al., 2020)*. Locations mentioned in the text are labelled here.*

2. Regional Setting and Environmental History

Dove Bugt is an embayment situated east of the southernmost outlets of the NGIS, Storstrømmen and L. Bistrup Bræ (Fig. 1b). Storstrømmen and L. Bistrup Bræ are two of the largest surge-type glaciers in the world (Higgins, 1991) with a surge periodicity of approximately 70 years (Mouginot et al., 2018). These two glaciers flow north and south, respectively, around the nunatak complex of Dronning Louise Land and merge in Borgfjorden (Fig 1b & 1c; Mouginot et al., 2018). The elongated island of Store Koldewey to the east of Dove Bugt largely shelters the embayment from the East Greenland Current. South of the bay is the sound Store Bælt, which is an outlet to the Greenland Sea.

West of Store Bælt, between Adolf S. Jensen Land and Dronning Margrethe II Land, is the west-east running Bessel Fjord (Fig. 1c). The western end of the fjord contains one of the two outlets of Soranerbræen, an outlet glacier that also connects to Dove Bugt to the north (Fig. 2). Several ice caps are positioned across the length of the fjord (Fig. 2 & 3), some of which have several generations of moraines and glaciofluvial outlets that enter the fjord. Colluvial fans and rivers have been observed across the length of the fjord in satellite images and while surveying the fjord. Multiple islands are located at the entrance of Bessel Fjord, the largest of which, Trums Ø, splits the entrance into two main inlets (Fig. 1c & 2). From the termination of

https://doi.org/10.5194/egusphere-2022-970
Preprint. Discussion started: 11 October 2022

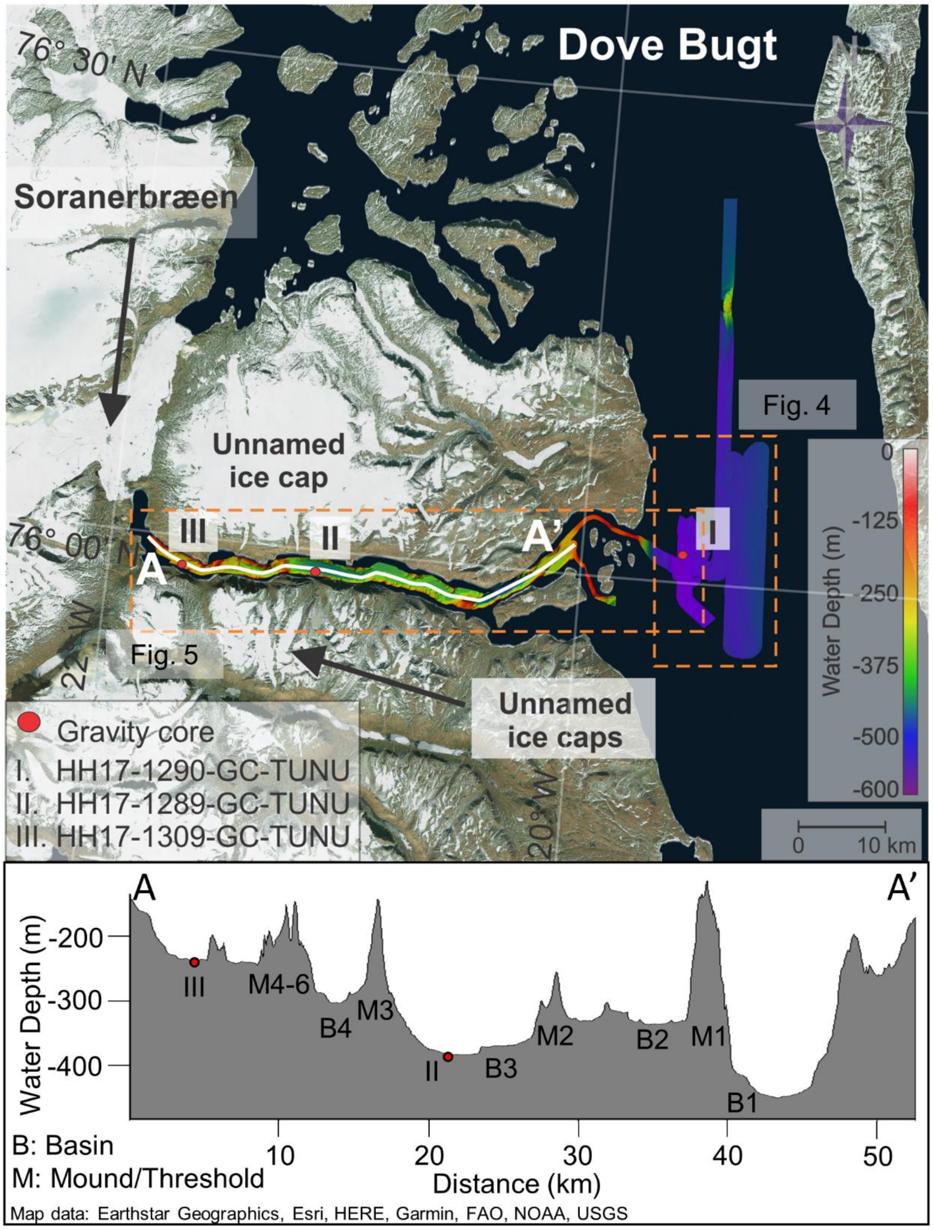

Figure 2. Study area with the bathymetric data showing the locations of the sediment cores presented in this study. The lower panel is a profile along the length of Bessel Fjord, A-A'. Sediment cores are labelled I, II and III. Satellite image is displayed using a World Imagery satellite image (Earthstar Geographics | Esri) made available through GlobalMapper.

https://doi.org/10.5194/egusphere-2022-970
Preprint. Discussion started: 11 October 2022

Figure 3. Image of an ice lobe from an ice cap near gravity core HH17-1289-GC-TUNU. Two sets of coarse-grained terminal morainal ridges are indicated by numbers and arrow. See Fig. 6b for the position of the modern ice lobe. The photograph was taken by Torger Grytå on a 2017 TUNU cruise.

Soranerbræen to the island of Trums Ø the fjord measures approximately 47 km in length. The width of the fjord ranges from 1.8 to 3.7 km.

Mega-scale glacial lineations (MSGL) identified along the continental shelf have been interpreted as evidence for the expanse of the GrIS to the shelf break during the LGM at this latitude (Laberg et al., 2017; Olsen et al., 2020). This is further supported by the presence of recessional moraines and grounding zone wedges identified across the continental shelf of Northeast Greenland, which suggests a complex deglaciation of the shelf area (Arndt et al., 2015, 2017; Laberg et al., 2017; Arndt, 2018; Olsen et al., 2020). Across the GrIS, deglaciation is believed to be asynchronous, with factors such as topography and local ice dynamics playing a large role with ice retreat in conjunction with climate change (Bennike & Björck, 2002; Funder et al., 2011; Ó Cofaigh et al., 2013; Hogan et al., 2016). Olsen et al. (2020) has suggested that deglaciation in the northeast may have occurred in two stages: first, an initial retreat as a result of eustatic sea level rise caused by melting ice at lower latitudes (Lambeck et al., 2014), followed by a melting phase driven by ocean warming.

Terrestrial studies of Dronnings Margrethe II Land, Germania Land and adjacent areas have identified a complex assortment of moraines that are believed to have formed during the Kap Mackenzie, Muschelbjerg, Nanok I and Nanok II stadials (Hjort, 1979, 1981; Hjort and Björck, 1983; Björck et al., 1994; Landvik, 1994). The exact ages of these stadials remain unclear (Table 1), yet Vasskog et al. (2015) suggests that the Milne Land moraines (referred to as G-II) formed during the late Younger Dryas (~12 ka BP) (Table 1).

https://doi.org/10.5194/egusphere-2022-970
Preprint. Discussion started: 11 October 2022

Table 1. Previously published stadial information for the Dove Bugt region as well as age estimates used in this study.

Stadials	**Studies**				**Age estimate used in this study**
	Hjort & Björck (1983)	*Funder et al., (1998)*	*Kelly et al. (2008)*	*Vasskog et al. (2015)*	
Nanok II	10.1-9.5 ka BP	Preboreal (ending at ca. 9.7 ka)	Younger Dryas and early Holocene (13-11.6 ka (G-III), 11.7-10.6 ka (G-II))	Close to Bølling–Allerød transition, and late Younger Dryas (~14 ka (G-III), ~12 ka BP (G-II))	Younger Dryas
Nanok I	Older than 14 ka, possibly between 15 and 19 ka				LGM or a readvancement during a deglaciation phase of the LGM
Nanok 0		~48 ka (Hjort, unpublished data)			
Muschelbjerg	Saalian (or older)?				Saalian (or older)?
Kap Mackenzie	Saalian (or older)?				Saalian (or older)?

The position of striations on Store Koldewey and lateral moraines on coastal slopes between Bessel Fjord and Haystack have been interpreted as evidence for ice flowing out of Dove Bugt and Bessel Fjord during the Muschelbjerg stadial, southwards through Store Bælt and turning eastwards around the southernmost mountains of Store Koldewey (Hjort, 1981). Early studies of the region noted glacial and glaciofluvial deposits (e.g. moraine plateaux, terminal moraines, eskers and sandurs) on Hochstetter Forland that are believed to have formed during this period (Hjort, 1979, 1981).

Lateral moraines and glacial striations oriented along the axis of Langsodal (also referred to as Langsødalen; Fig. 1c), a nearby valley south of and sub-parallel to Bessel Fjord, have been interpreted as evidence for glacial confinement within the valley during an undifferentiated Nanok stadial (Hjort 1979; Hjort, 1981). This differs from striations that have also been identified in the valley along more weathered surfaces that are oriented in a southwestern direction (Hjort, 1979).

On terrestrial areas, cosmogenic nuclide dates collected from Store Koldewey suggest that the region was deglaciated by 12.7 ka BP (Skov et al., 2020). Findings from macrofossil remains (Bennike & Björck, 2002) and lacustrine sedimentary records (Cremer et al., 2008) suggest that coastal regions were deglaciated in a ~1500 year span after the start of the Holocene (Klug et al., 2016). To the north of Store Koldewey, a minimum date for deglaciation in Germania Land

https://doi.org/10.5194/egusphere-2022-970
Preprint. Discussion started: 11 October 2022

of 9.5 ka BP has been proposed, whereas to the south in southern Dronning Margrethe II Land, a minimum date of 11.2 ka BP has been suggested (Bennike & Weidick, 2001).

Lake studies on aquatic organisms at Duck Lake and Hjort Lake on Store Koldewey (Fig. 1c) indicate that the island was at its warmest between ~8 and 4 ka, (Wagner et al., 2008; Klug et al., 2009; Schmidt et al., 2011), although findings from Melles Lake (Fig. 1c) suggest that the earliest onset of warmth during the Holocene may have occurred at ~ 10 ka (Klug et al., 2009; Briner et al., 2016). On Hochstetter Forland (Fig. 1c), pollen assemblages from Dødis Sø, Peters Bugt Sø and Ailsa Sø suggest that the temperatures were at their highest between 8.8 and 5.6 (Björck & Persson, 1981; Björck et al., 1994). These findings indicate that the HTM was not uniform across East Greenland, as also described by Briner et al. (2016).

3. Material and Methods

Swath bathymetry and three sediment cores were collected in southwestern Dove Bugt and Bessel Fjord during an expedition aboard RV *Helmer Hanssen* of UiT The Arctic University of Norway in September 2017, being part of the TUNU program (Fig. 2; Christiansen, 2012). The swath bathymetry data was obtained using a Kongsberg Maritime Simrad EM 302 multibeam echo sounder. It was gridded using Petrel software, and geomorphological interpretations were made using Global Mapper 18. Surfaces were developed using a 5x5m grid cell size while a surface created from an International Bathymetric Chart of the Arctic Ocean (IBCAO) dataset 4.0 with a 200x200m grid cell size (Jakobsson et al., 2020).

Two soft sediment gravity cores were retrieved from Bessel Fjord (HH17-1289-GC-TUNU & HH17-1290-GC-TUNU) and one southwest of Dove Bugt in the sound Store Bælt (HH17-1309-GC-TUNU) (Fig. 2 & Table 2). Prior to splitting the cores, physical properties were measured using a GEOTEK Multi Sensor Core Logger (MSCL-S). The cores were placed in the laboratory for 24 hours prior to obtaining physical measurements to ensure that each core temperature reached equilibrium with the laboratory to avoid distorting p-wave values (Weber et al., 1997).

Table 2. Information on the position, water depth and recovery length of each gravity core. Note that the core names are abbreviated in the text.

Location	**Inner Bessel Fjord**	**Mid-Bessel Fjord**	**Southeastern Dove Bugt**
Coring station	HH17-1290	HH17-1289	HH17-1309
Latitude [N]	75° 58' 34.5907"	75° 58' 11.4928"	76° 01' 34.0387"
Longitude [W]	21° 07' 13.1055"	21° 41' 48.0278"	19° 34' 31.3190"
Water depth [m]	372	225	512
Recovery [cm]	534.5	245.5	474.55

A GEOTEK MSCL X-ray Computed Tomographic imaging machine was also used to scan the unopened core sections to create X-ray radiographic images. After each core was split and cleaned, the characteristics of the sedimentary surface were logged (i.e. structures, bioturbation, grain size, lithological boundaries, etc.), sediment color was noted using the Munsell Soil Color Chart and lithofacies were assigned based on Eyles et al. (1983) classification system. X-ray fluorescence (XRF) data, as well as colored images of the core sections, were then obtained using an Avaatech XRF core scanner. Ca/Fe elemental ratios have been added to core logs as this ratio can be used to distinguish between biogenic

https://doi.org/10.5194/egusphere-2022-970
Preprint. Discussion started: 11 October 2022

carbonate and detrital clay content (Rothwell et al., 2006). It is worth noting that sediment cores collected near areas of terrestrial runoff have the potential to introduce non-biogenic calcium into the sampled sediment which can dilute the signal of the biogenic carbonate. While runoff from glaciers and rivers have the potential to impact the cores in Dove Bugt and Bessel Fjord, what is known about the chemical composition of the surrounding rocks in Bessel Fjord (Henriksen and Higgins, 2009) suggests that the introduction of terrestrial calcium would only likely minimally impact Ca/Fe ratios. Therefore, while it is important to consider the potential influence of terrestrial calcium, at this time their impact is believed to be negligible.

Molluscs and benthic foraminifera were recovered from each core for the purpose of radiocarbon dating. Two adjacent 1 cm thick sediment slices were sampled from select positions across cores HH17-1290 and HH17-1309. Samples were then wet sieved at 1 mm, 100 µm and 63 µm meshes, respectively. Benthic foraminifera from the 100-um size fraction were extracted for radiocarbon dating. Radiocarbon dating was carried out at the MICADAS radiocarbon laboratory at Alfred Wegener Institute, Helmholtz Centre for Polar and Marine Research, Germany. The radiocarbon dates were calibrated using the Calib 7.1 software (Stuiver and Reimer, 1993) applying the MARINE13 calibration curve (Reimer et al., 2013) and a ΔR of 162 ± 27 years suggested for this region (Håkansson, 1973; Funder, 1982).

A Beckman Coulter LS 13 320 Multi-Wavelength Laser Diffraction Particle Size Analyzer was used to perform sediment grain size analysis. Sediment was sampled in mostly 10 cm intervals across HH17-1309, where samples taken from the other two cores were selected from specific positions. Samples were treated in HCl and H_2O_2 and a pre-heated VWB 18 Thermal Bath. Samples were then cleaned using distilled water, placed through multiple runs through a centrifuge and heated in an oven to remove water content. Approximately 0.2 grams of sediment were then separated and placed in a container with 20 ml of water and moved to a shaking table for over 48 hours. A few drops of Calgon were added to each sample, which was then placed into a Branson 200 ultrasonic cleaner for ~7 minutes and shaken briefly before being poured through a >2 mm mesh and into the particle size analyzer. Grains between the size of 0.4 µm and 2000 µm were counted and underwent three separate runs. GRADISTAT Excel-software was used to calculate the mean of the three runs. Sediment names used in reference to this analysis are based on Folk (1954) and mean grain size from the methodology published by Folk & Ward (1957).

4. Results

4.1. Seafloor landforms in SW Dove Bugt (Store Bælt)

4.1.1. Elongated Lineations - Glacial Lineations

Slightly curved sub-parallel lineations, oriented sub-parallel to the axis of Dove Bugt, are the most pronounced landforms in this part of the study area. They are oriented N-NW in the south and N-NE in the north (Fig. 4). The most frequently identified positive lineations (ridges) are 35-50 m in width, <1-3 m in height and between 1 and 10 km in length. Length to width ratios are frequently >10:1. At elevations shallower than 435 m depth, near the center of Store Bælt, the lineations are wider (e.g. 60-150 m wide), and occasional merging and overlapping of lineations occur (Fig. 4e). Wider lineations, often identified in the southern section of the study area (Fig. 4b), have also been identified with widths, lengths and heights ranging from 200-650 m, 3 – 8 km and 4.5 – 15 m, respectively. Length to width ratios here are 7:1 to >10:1. Some of the larger lineations are superimposed by smaller lineations. Lateral ridges have also been

https://doi.org/10.5194/egusphere-2022-970
Preprint. Discussion started: 11 October 2022

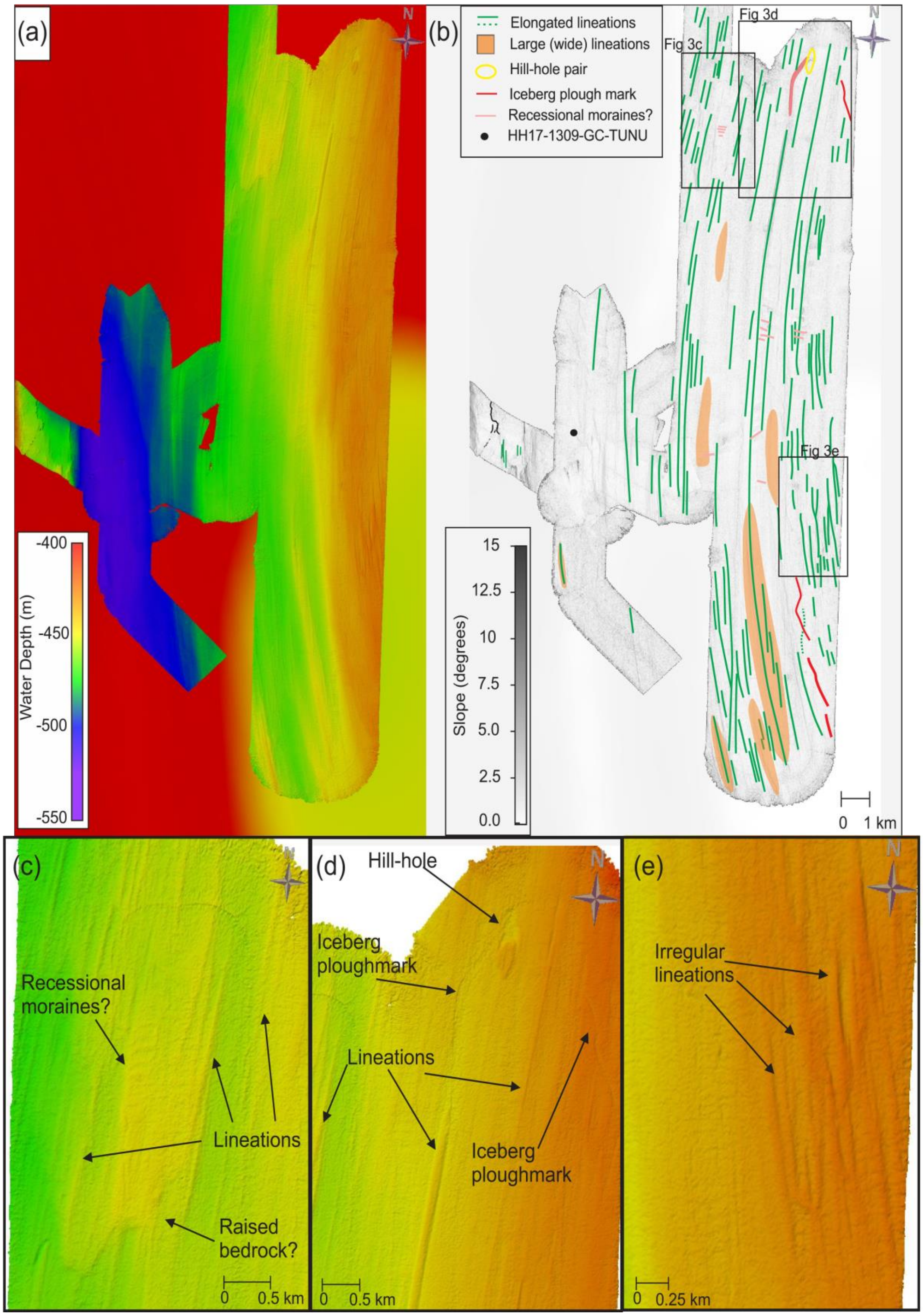

Figure 4. Bathymetric maps from SW Dove Bugt. (a) Seafloor relative to water depth with IBCAO 4.0 displayed in the background (Jakobsson et al., 2020). *(b) The main landforms and slope angles of the seafloor in SW Dove Bugt. Locations of Figs. 4c-e are indicated. (c) Bathymetry of the northwestern section of the study area. (d) Bathymetry of the northeaster part of the study area. (e) Bathymetry of the eastern part of the study area showing irregularly shaped glacial lineations.*

https://doi.org/10.5194/egusphere-2022-970
Preprint. Discussion started: 11 October 2022

identified in clusters overprinting the lineations (Fig. 4c), where furrows have been found cross cutting lineations (Fig. 4d). Lateral ridges measure 0.5 to 2 m in height and are spaced approximately 45 to 250 m apart from each other.

These elongated lineations are interpreted as glacial lineations (e.g. Ó Cofaigh, 2005). The thinner, more common lineations (with length/width-ratios >10:1) have been interpreted as mega-scale glacial lineations (MSGL), and such landforms are commonly associated with palaeo-ice stream environments (e.g. Stokes & Clark, 2001). While the mechanism behind the formation of these features are still being debated, some authors have suggested that they may have formed through meltwater flooding (Shaw et al., 2008), groove-ploughing (Clark et al., 2003) or the transverse flow in basal ice (Schoof and Clarke, 2008). King et al. (2009), who viewed the formation of MSGL in real time in West Antarctica favored aspects of the dilatant till instability model, but with till properties that could explain ribbed moraine formation and the development of these landforms on a decadal timescale. Sets of ridges that overprint the glacial lineations have been interpreted as recessional moraines, where furrows have been interpreted as iceberg plough marks.

4.1.2. Depression and Mound- Hill-Hole Pair

In northern Store Bælt, a 200 by 450 m wide, 3-4 m deep depression has been identified next to a mound with a width and height of 235 by 450 m and 3-4 m, respectively (Fig. 4d). The depression overprints N-S trending lineations, although the mound contains lineations on its surface.

This depression and mound have been interpreted as a hill-hole pair. These landforms can form when ice-thrust rafts of sediment are removed from the bed by cold-based, slow-flowing ice that transports the sediment that was once in the depression (Hogan et al., 2010; Klages et al., 2013, 2015). In this instance, a south bound ice stream may have removed frozen sedimentary material and deposited it further south.

4.2. Sea floor landforms in Bessel Fjord

4.2.1. Large scale geomorphology

Bessel Fjord contains a variety of basins that are separated by different styles of sills (Figs. 2, 5 & 6). The outermost sill is at the fjord's entrance, and it commonly ranges in depth from 50 to 200 m, with sections reaching above the water surface as there are islands in the fjord entrance. Four large basins that are elongated in a west-east direction have been identified in Bessel Fjord (B1-B4). The deepest basin, Basin 1 (B1), is the closest to the fjord entrance and is separated from basin 2 (B2) by a >215 m high sill (M1) that is steeper to the east (Figs. 2 & 5). Basin 3 progressively deepens westwards, with a maximum depth of 380 m. A ~70 to 160 m asymmetrical sill (M3; Figs. 2 & 5) that is steeper on its east side separates Basin 3 from basin 4. Basin 4 is the shallowest basin (~280-300 m) and is adjacent to multiple smaller basins that are primarily at lower points of elevation. The fjord also contains smaller basins that are raised relative to the average seafloor depth (Fig. 6e). Features interpreted as bedrock mounds have also been identified in other sections of the fjord (Figs. 5 & 6). Along the fjord sides, landforms from sediment reworking including slide scars, channels and gullies have also been observed Fig 6b.

4.2.2. Linear Ridges Oriented Along Fjord Axis- Glacial Lineations

Oriented along the fjord's axis (or at times slightly oblique to it), linear features have been identified in the inner and middle of the fjord, as well as a single lineation on the outer part of the fjord (Figs. 5 & 6). They range in size from 100 to 1000 m in length and ~3 to 9 m in height,

https://doi.org/10.5194/egusphere-2022-970
Preprint. Discussion started: 11 October 2022

although some that are as high as 80 m have been identified in the inner fjord. Their morphologies vary throughout the fjord, and their length to width ratios range from 2:1 to 5:1. Most ridges slope towards the outer fjord, although some slope in the opposite direction or have an irregular or flat top. They appear both independently in connection with inferred bedrock highs, and in clusters in flat lying areas of basin 3. These ridges have been interpreted as glacial lineations, and they are thus indicating the direction of former glacier flow.

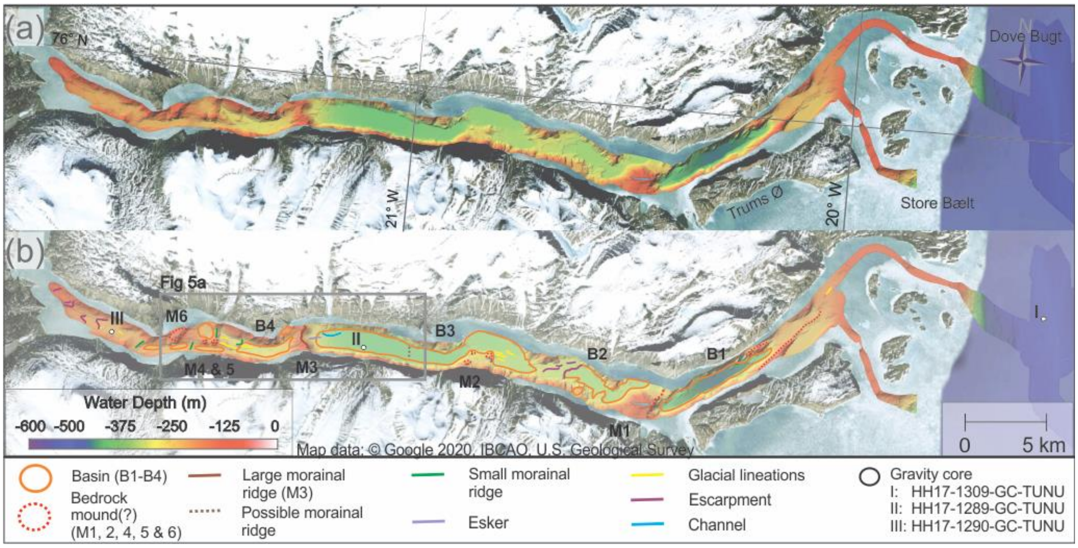

Figure 5. (a) Bathymetric map of Bessel Fjord. (b) A map of mapped features in Bessel Fjord. Satellite images obtained from Google Earth (© Google 2020).

4.2.3. Transverse Ridges- Moraines

Several transverse ridges have been identified in the inner and central portion of the fjord, oriented perpendicular to the fjord's axis (Figs. 2, 5 & 6). The ridges in the inner most position of the fjord tend to largely conform to the topography (i.e. between bedrock mounds and the fjord sidewalls) and are, at times, the threshold between sub-basins (Fig. 6). The width and length of ridges range from 150 to 600 m and 120 to 500 m, respectively, where their heights are between <5 to 58 m.

A particularly large, asymmetrical transverse ridge that spans the width of the fjord, is situated between Basin 3 and 4 (M3; Figs. 2 & 6d). This ridge is ~1.5 km in width and between 72 to 162 m in height. It contains a crescent shape in aerial view and is concave towards the mouth of the fjord. A large threshold with a 1.8 km width and a > 215 m height also separates basin 1 and 2 (M1; Figs. 2 & 5). This feature is ~150m shallower in the north and dips steeply into basin 1.

The transverse ridges have been interpretation as moraines, which would have formed during glacial stillstands or readvancements during the retreat of a grounded tidewater glaciers margin. While the large transverse ridge M3 is believed to be a moraine, it is considered more likely that M1 is a bedrock mound based on its morphology. The smaller transverse ridges are interpreted as recessional moraines. Smaller moraines have the potential to form at ice margins annually (Lyså & Vorren, 1997; Dowdeswell et al., 2016) and have been observed with a variety of sizes and morphologies on the NE Greenland shelf (e.g. Winkelmann et al., 2010).

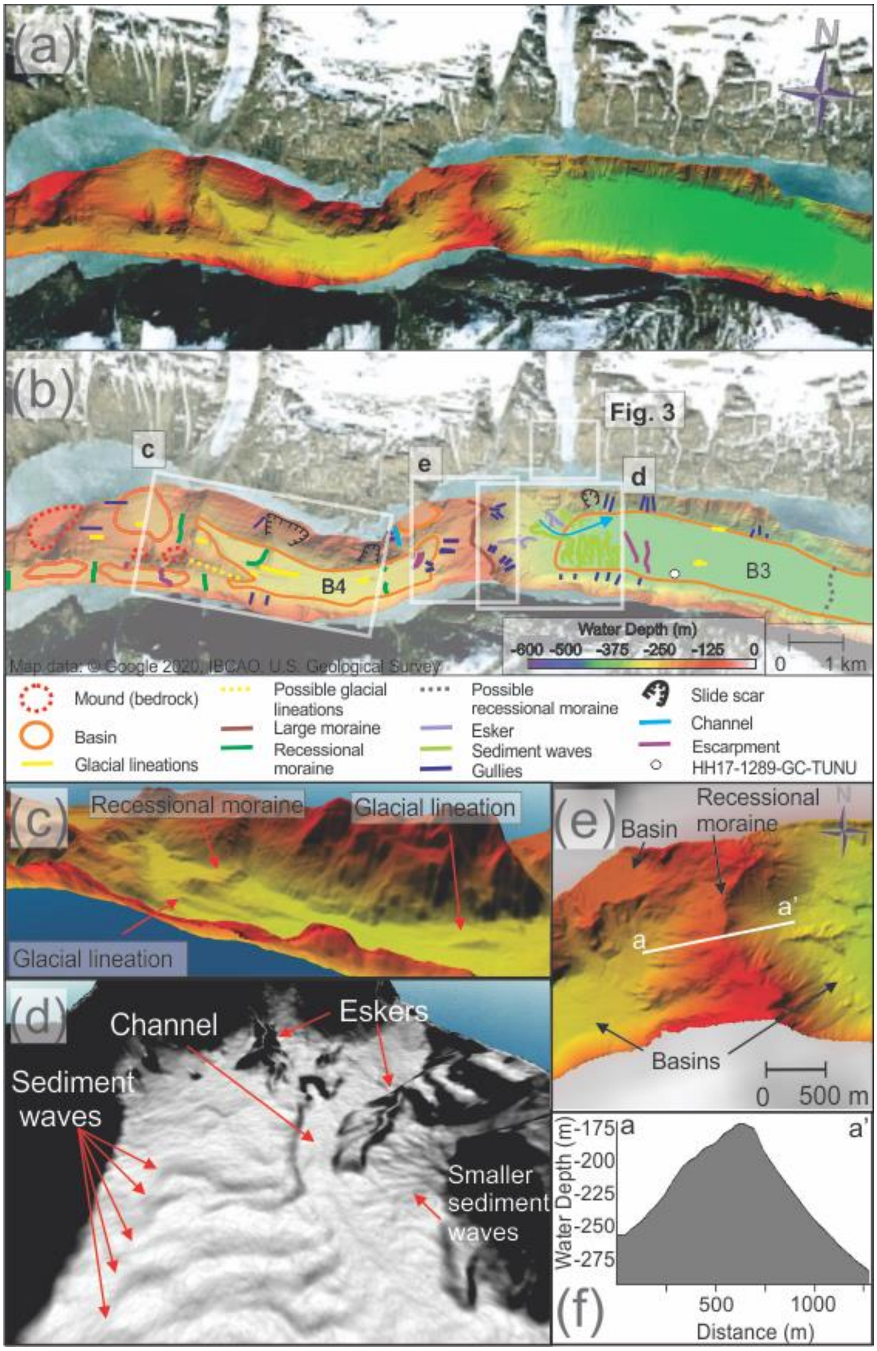

Figure 6. (a) Mapped sections from inner to middle Bessel Fjord. (b) Glacial lineations in Basin 4 (B4). Background images used for 6a & 6b obtained from Google Earth (© Google 2020). (c) Eskers, sediment waves and a channel in Basin 3 (B3). (d) A large moraine (M3) between B3 and B4. Note the raised sub-basin to the west and esker to the east. (e) Profile across the large recession moraine (M3).

4.2.4. Sinuous Ridges- Eskers

Sinuous ridges, oriented parallel or oblique to the fjord's axis, occur in basin 3 (Figs. 5, 6b, 6d &6e). These features have widths and lengths of 50 to 120 m, 350 to 800 m, respectively and heights of 10 to 15 m. The most pronounced examples of these ridges have been observed east of the large recessional moraine that has been previously discussed (Fig. 6e).

These sinuous ridges have been interpreted as eskers. These landforms form from sediment infill of subglacial and englacial conduits. They frequently form in the direction of former ice flow and often form during terminal stages of glaciation, and are therefore associated with moraines (Shreve, 1985). They vary in size depending on the glacial drainage pattern, as well as a number of other factors, however eskers identified within Bessel Fjord appear smaller than those identified in studies in Canada, the UK and Kola Peninsula in Russia (Storrar et al., 2014)

4.2.5. Wavy Transverse Ridges- Sediment Waves

Adjacent to the two eskers in Basin 3 are a series of wavy transverse ridges to the east of a large recessional moraine (Figs. 5, 6b & 6d). These features occupy an area of ~500 by 1500 m and contain small ridges and flat areas that slope at an angle of 3 to 6° to the east. Each wave "crest" is ~50 to 100 m apart, although some appear to begin only halfway through the width of the area, where others occupy the entire width, north to south. These waves are crosscut by a channel to the north (Fig. 6d). North of this channel similar features with a wavy morphology occur, although these are substantially smaller.

These wavy transverse ridges have been interpreted as sediment waves. Sediment waves found associated with deltaic and glacifluvial deltaic systems have been associated with retrogressive slope failures, gravity-induced sediment creep and/or the migration of sediment waves upslope (Cartigny et al., 2011; Hill, 2012; Stacey and Hill, 2016). Alternatively, given the position of the smaller wavy transverse ridges to the ice cap on Ad. S. Jensen Land (Figs. 1 & 2) and the larger ridges to the large moraine to the west (Figs. 5 & 6) it is also possible that these ridges are sets of moraines. Recessional moraines have been identified in the vicinity of eskers in Spitsbergen fjords (Ottesen et al., 2008; Kempf et al., 2013), which may account for the smaller wavy transverse ridges. The larger wavy transverse ridge do also resemble thrust moraines identified by Forwick et al. (2010). Further work may be required in the evaluation of these features. Please see Table 3 for a full list of observed landforms.

4.3. Lithostratigraphy

Three gravity cores were retrieved from the study area. Gravity core HH17-1309 was collected in western Store Bælt, just outside of Bessel Fjord. This core has sampled from a N/NW-S/SE oriented depression that contains iceberg ploughmarks and a MSGL and includes lithological units of mud and a diamict (Figs. 7a-c). Gravity core HH17-1289 was collected in the middle of the Bessel Fjord, near the southern sidewall of the fjord. The core is located directly east of the above-mentioned sediment waves on the distal part of the pronounced transverse ridge. Nearby, a modern ice cap fed glacifluvial channel is observed in satellite imagery, likely with a delta at its fjord termination. This core contains a substantially higher sand content than other cores collected in the region (Units 2.2-2.4). The gravity core HH17-1290, comprising mostly muddy deposits (Units 3.1-3.3), was collected within the inner fjord. The gravity core is west of the basins and thresholds observed in this study and is the closest core to Soranerbræen (located about 9.7 km east of the glacier) (Fig. 7).

https://doi.org/10.5194/egusphere-2022-970
Preprint. Discussion started: 11 October 2022

Table 3. Overview of observed landforms in southern Dove Bugt and Bessel Fjord.

Region	Description	Width	Length	Height	Notable Feature	Interpretation
Dove Bugt	Elongated lineations	35-50 m	~1->10 km	<1-3 m	Roughly N-S	Glacial Lineations
	**Wide*	200-650 m	3.8 to 8.8. km	4.5-15 m		
	Depression and mound	200 m	450 m	3-4 m	Mound to the south of the depression	Hill-hole pair
	Furrows (scour marks)	~40-100 m	<100-200	3-5 m	Irregular	Iceberg plough marks
	Transverse ridges	150-400 m	~30-100 m	0.5-1 m	Roughly W-E	Recessional moraines
Bessel Fjord	Linear ridge	45-350 m	100-1000 m	3-9, 80 m	Parallel to the fjords axis	Glacial Lineations
	Transverse ridges	150-600 m	120- 500 m	<5-58 m	Perpendicular to the fjords axis	Recessional moraines
	**Large ridge (M3)*	1485 m	600-1600 m	72 to 162 m		Moraine
	Sinuous ridges	50-120 m	350-800 m	10-15 m		Esker
	Wavy transverse ridges	400-700 m	~45-100 m	2-5 m	Perpendicular to the fjords axis	Sediment wave
	Elongated depression	~200 m	~1 km	6-8 m		Channels
	Chute	~20-100 m	60-400 m	1-15 m		Gullies

4.3.1. Facies

Facies 1 – Laminated Mud (Fl, Fl-d & Fl/m-d)

Facies 1 consists of laminated mud (Fl) and laminated mud with dropstones (Fl-d) and have been observed in all three gravity cores (Figs. 7, 8a, 8d & 8f)). Laminations are composed of either mud or very fine sand. Mud laminations with finer laminations have also been identified in Unit 3.2 (100-200 cm; Fig. 7a, Fl/m-d). Microfractures have also been identified within this facies (Fig. 8f).

Wet-bulk density measurements tend to increase with depth in some sections of this facies (e.g. 87-350 cm in HH17-1309), suggesting normal sediment consolidation. However, a stagnation or decrease in wet-bulk density with depth in other sections (e.g. below ~350 cm in HH17-1309) suggests less or no consolidation. The magnetic susceptibility generally tends to increase with depth in HH17-1309 and in Unit 3.2 in HH17-1290, however the remainder of this facies in HH17-1290 (Unit 3.1) remains relatively stable to the base of the core. Notable positive peaks have been identified at 110 and 140 cm in HH17-1309 and measurement fluctuations occur in HH17-1289. Peaks in magnetic susceptibility may reflect the introduction of turbidites or clasts where fluctuations may reflect shifts in sediment provenance.

Muds with sand laminations are believed to have formed through a combination of ice-proximal suspension settling from overflow plumes and turbidity-current activity (underflows). The rhythmically laminated muds are believed to have formed from ice-proximal suspension settling from turbid overflow plumes. Similar laminated sediments have been identified by Cowan et al. (1999) in Alaska and Forwick & Vorren (2009) in Svalbard. Large clasts have been interpreted

https://doi.org/10.5194/egusphere-2022-970
Preprint. Discussion started: 11 October 2022

as ice rafted debris (IRD) and the formation of microfractures may have been caused by soft sediment deformation, possibly including hydrofracturing, from subglacial or proglacial processes. Similar soft, marine sediment deformation from a glacial environment has previously discussed by Passchier (2000) in Antarctica.

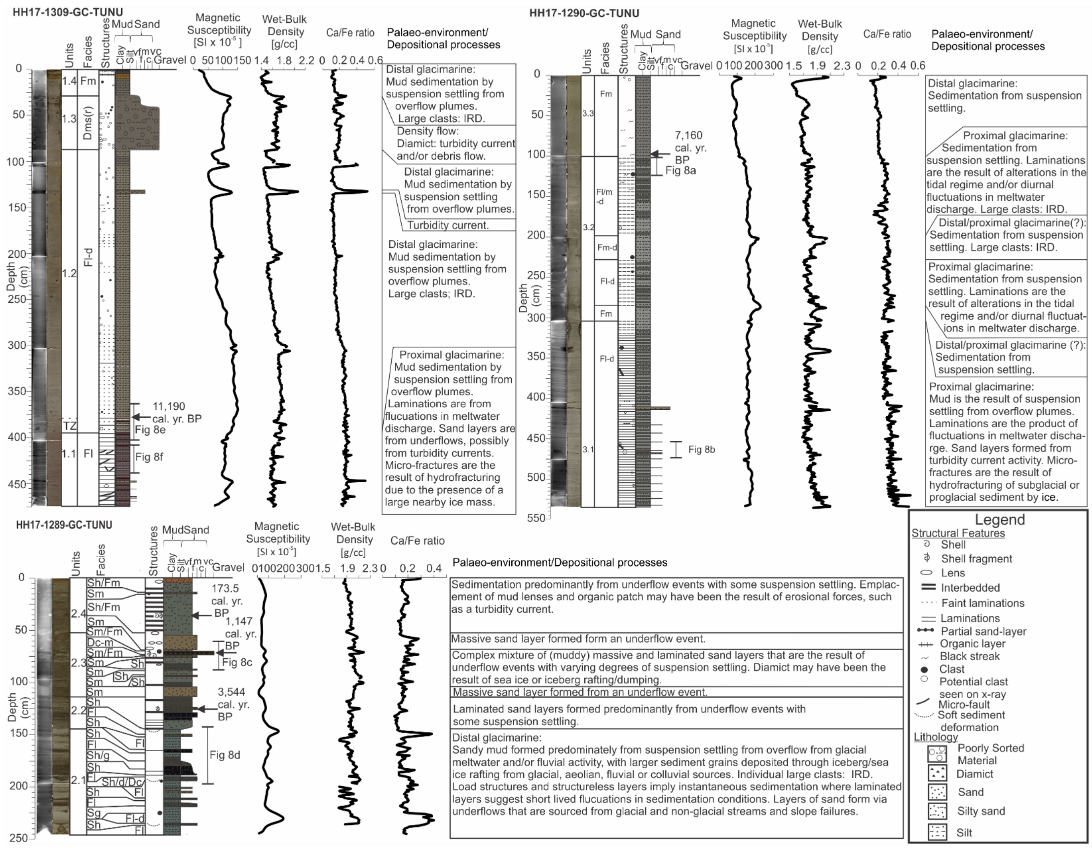

Figure 7. Lithological core logs of the three gravity cores with x-ray images, core photos, unit divisions, facies, structures, magnetic susceptibility wet-bulk density and Ca/Fe ratios displayed. TZ in HH17-1309-GC-TUNU stands for "Transition Zone".

Facies 2 – Massive Mud (Fm & Fm-d)

The second facies consists of massive mud with or without dropstones and can be found in the inner fjord core HH17-1290 and the Store Baelt core HH17-1309 (Fig. 7). In HH17-1290 this appears downcore between sections of Facies 1 as well as in the topmost unit, Unit 3.3. The magnetic susceptibility gradually increases downcore in this facies in Unit 3.3. Further down core, in Unit 3.2, this facies is associated with a downwards trend in magnetic susceptivity following peaks in measured reading. Wet bulk density values roughly mirror these trends. In HH17-1309 massive mud units have been observed in Unit 1.4, where magnetic susceptibility and wet bulk density values increase downcore.

This facies is interpreted as being the result of suspension settling from overflow plumes and is believed to have been deposited in an ice-distal glacimarine environment with varying input from

https://doi.org/10.5194/egusphere-2022-970
Preprint. Discussion started: 11 October 2022

IRD (i.e. Boulton & Deynoux, 1981). Sediment may be sourced from a single location (i.e. Soranerbræen) or more than one location (e.g. local ice caps) in an ice-distal glacimarine environment with limited iceberg or sea-ice rafting.

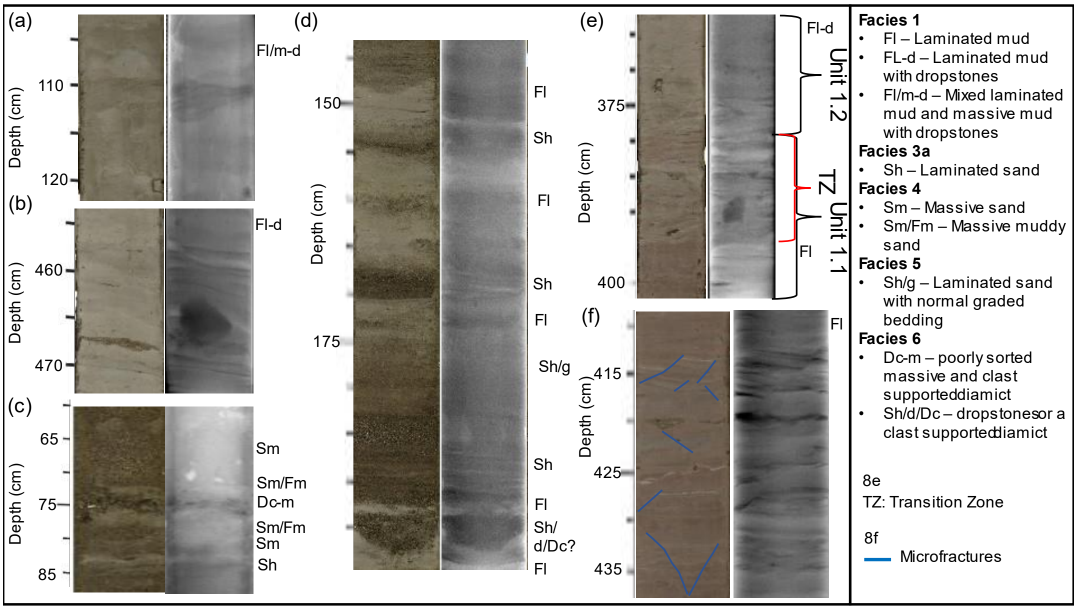

Figure 8. Photographic and x-ray images of sections of the three gravity cores (a-f). Corresponding facies codes can be found to the right of each image.

Facies 3a – Laminated Sand (Sh)

Facies 3a consists of sections of sand with horizontal sand laminations. This facies has been predominantly observed in the mid-fjord core, HH17-1289-GC-TUNU (Figs. 7 & 8d). These sections consist of fine to medium grained sand that range in thickness and colors. This facies does not contain uniform magnetic susceptibly or wet-bulk density readings as it has been found in association with low and high peaks of both parameters as well as values that are near the average for the core.

This facies is interpreted as being deposited from turbidity currents, possibly underflows that are either sourced from glacial or non-glacial streams and slope failures. Uniform layers may indicate a single, rapid event, where shifts in grain size and color may be the result of short-lived fluctuations in sediment input.

Facies 3b – Laminated Muddy Sand (Sh/Fm)

Facies 3b represents sections of sand with faint horizontal laminations as well as a large quantity of clay material interspersed throughout with faint laminations. This has been observed in HH17-1289 at the topmost unit in the core, Unit 2.4 (Fig. 7). Magnetic susceptibility is relatively uniform in this facies, where the wet-bulk density tends to decrease up core. Sediment grain size analysis of a single sample from this facies revealed that the sediment is composed of 56.3% sand and 43.7% mud. A "patch" of black organic material (i.e. plant material and shells) was also identified within this unit.

https://doi.org/10.5194/egusphere-2022-970
Preprint. Discussion started: 11 October 2022

This complex facies is believed to have formed predominantly from underflow events, sandy – muddy turbidites, alternatively sandy turbidites with additional input from suspension settling. Similar deposits have been observed in Balsfjord, Norway although without lamination and possibly a higher mud content (Forwick and Vorren, 1998).

Facies 4 – Massive Sand / Massive Muddy Sand (Sm & Sm/Fm)
Facies 4 contains sections of massive sand (Sm) as well as massive sand with a large amount of clay content (Sm/Fm). This facies is predominantly found in Unit 2.3 (and to a much less extent, Unit 2.4) in HH17-1289 (Fig. 7). Sections of massive sand have been found in association with mud lenses and often contain horizontal sand layers (Sh) above and below it. Slight increases and decreases in magnetic susceptibility values have been observed within this facies.

The facies is believed to have developed through rapid deposition as well as deformation of Facies 3a & b. According to this interpretation, the mud lenses observed in this facies were once layers/lamina that became deformed due to the sand – mud density contrast. Massive sand deposits with similar characteristics have also been observed in an Alaskan fjord near Muir Glacier (Cowan et al., 1999).

Facies 5 – Sand with Normal Graded Bedding (Sg & Sh/g)
Facies 5 is used to depict sediment that contains normal graded bedding (Sg) or appear to have clear horizontal laminations and have normal grained bedding (Sh/g). This has been observed in layers of sediment within Unit 2.1 of HH17-1289 (Figs. 7 & 8d). As normal graded sands have been observed in the A layer of the Bouma sequence, it is possible that these layers formed from turbidity currents during underflow events.

Facies 6 – Diamicts (Dc, D-m, Dc-m, Dms(r) & Sh/d/Dc)
Facies 6 contains a variety of different diamicts observed within the mid-fjord core HH17-1289 and the Store Baelt core HH17-1309. In HH17-1289 this includes a 3.5 cm poorly sorted massive and clast supported diamict (Dc-m) in the middle of Unit 2.3 (Figs. 7 & 8c), and a horizontally laminated layer of sand that that is either accompanied by dropstones or a clast supported diamict (Sh/d/Dc) (Figs. 7 & 8d). It is inferred that they are the result of sea ice or iceberg rafting/dumping. Within HH17-1309 there is a substantially larger, sharp based, matrix-supported diamict, stratified in its upper part (Dms(r)) in Unit 1.3 (Fig. 7). Based on these characteristics, this diamict has been interpreted as a density flow deposit, likely a debris flow deposit that is overlain by (part of) a turbidite.

4.3.2. Chronology and sedimentation rates
Shell and shell fragments were recovered from HH17-1289 for radiocarbon dating. At 34 cm depth, a semi-spherical path of organic content was identified, containing two intact *Yoldiella lenticula*, a shell fragment and plant material. Additionally, at 71 cm depth, a large 3 cm half of a *Hiatella arctica* shell was collected for dating, and shell fragments were recovered from a depth of 125 cm for the same purpose. These shells yielded radiocarbon ages of 174, 1,147 and 3,544 cal yr. BP, respectively (Table 4).

Cores HH17-1290 and HH17-1309 were subsampled for foraminifera material at four positions. Calcareous benthic species, which were rare, were used for dating and include predominantly *Melonis barleeanus* as well as *islandiella norcrossi*, but in substantially smaller quantities. In HH17-1309, at a depth of 377 cm *islandiella norcrossi* (rare to common) & *stainforthia feylingi* (rare) and a planktonic species were identified immediately above the transition zone between deformed (below) and undeformed sediments (above). Radiocarbon dates for the HH17-1309 sample yielded an age of 11,190 cal yr. BP where the sample from HH17-1290 yielded an age of 7,160 cal yr. BP (Table 4).

Table 4. Radiocarbon dates, calibrated dates, and associated linear sedimentation rates.

Coring station	Sampling Depth [cm]	Lab nr.	Species	^{14}C age BP	Cal yr BP Calib 7.10 1σ range	Cal yr BP Calib 7.10 2 σ range	Cal yr BP Calib 7.10 1 σ mean	Linear sedimentation interval [cm]	Linear sedimentation rate [cm/ka]
HH17-1309-GC-TUNU	377	5157.1.1	Mixed benthic foraminifera	10,357±95	11,075-11,308	10,921-11,592	11,190	0-377	33.69
HH17-1289-GC-TUNU	35	5154.1.1	*Yoldiella lenticula*	688±34	103-244	46-262	174	0-35	201.73
HH17-1289-GC-TUNU	71	5155.1.1	*Hiatella arctica*	1,747±28	1,096-1,208	1,047-1,247	1,147	35-71	31.39
HH17-1289-GC-TUNU	125.5	5156.1.1	Bivalve frag.	3,809±36	3,481-3,607	3,433-3,678	3,544	71-125.5	15.38
HH17-1290-GC-TUNU	97	5158.1.1	Mixed benthic foraminifera	6,800±80	7,059-7,258	6,943-7,340	7,160	0-97	13.55

Linear sedimentation rates were calculated assuming modern sediments are at the core top (Table 4). Sedimentation rates of ~15 cm/ka, ~31 cm/ka, & ~201 cm/ka were calculated for core HH17-1289 at 71-125.5 cm, 35-71 cm, and 0-35 cm, respectively. These results reveal an increase in the sedimentation rate towards the present. However, as this core includes multiple deposits from turbidity currents (i.e., reworked deposits), linear sedimentation rates in core HH17-1289 should be treated with caution. An average, linear rate of ~13 cm/ka was calculated for the interval of 0-97 cm in core HH17-1290 and an average, linear rate of ~33 cm/ka was also obtained for the large interval of 0-377 cm in core HH17-1309. These linear rates are lower, up to an order of magnitude, when compared to the Kejser Franz Josef Fjord system ~400 km south of the study area (Olsen et al., 2022). The origin of this observed difference must await further studies.

4.3.3. Ca/Fe elemental ratios

Large scale trends in Ca/Fe elemental ratios in core HH17-1290 in inner Bessel Fjord, and core HH17-1309 in the Dove Bugt, are relatively stable showing a slight increasing trend downcore (Fig. 7). This differs from the mid-fjord core, HH17-1289, which is more complex and does not contain a single trend. The topmost section of HH17-1290 and HH17-1289 do notably contain large peaks in Ca/Fe ratios that strongly decrease a few centimeters into each core. Minor

https://doi.org/10.5194/egusphere-2022-970
Preprint. Discussion started: 11 October 2022

peaks increase in frequency downcore in HH17-1290 as the presence of laminations increase. In HH17-1309, increased values are also observed in larger sand laminations, sand layers and diamict near the top of the core. Minor fluctuations occur throughout HH17-1289, often with shifts in ratio values occurring between different layers. This may indicate that within these cores minor fluctuations may be the result of changes in sediment provenance. This, however, is more complicated in HH17-1289, as many of the layers are reworked sediment (turbidites).

5. Discussion

5.1. Ice Sheet advance

The appearance of glacial lineations in Bessel Fjord suggest that the fjord was once fully glaciated, which is in accordance with the inferred shelf break-terminating ice sheet inferred for the LGM from other studies (e.g. Laberg et al., 2017; Olsen et al., 2020) (Fig. 9a & 9b). Ice that filled the fjord is believed to most likely be from the modern Soranerbræen glacier but may have also included ice caps and other branches of inland ice. Additionally, deep basins and base-level flattening within the fjord likely originate from multiple (pre-LGM) ice advances into the fjord (e.g. Barnes et al., 2016).

Glacial lineations are believed to have formed during the LGM or during an ice readvance in the deglaciation. Onshore and south of Bessel Fjord, two sets of striations identified in Langsødalen (Hjort, 1979, 1981) may suggest that this valley experienced two glaciation events during this period (Fig. 1c). Striations, and lateral moraines, found along the fjord axis may be the result of the east-west movement of ice through the valley, where SW oriented striations may be the result of Storstrømmen encroaching also onto terrestrial areas. Hjort (1981) suggested that striae on Haystack may indicate that ice flow was dominant from the north during the Nanok Stadial but ice pressure from Langsødalen dominated later after deglaciation begun. Thus, it is possible that ice masses drained through both Bessel Fjord and Langsødalen during full-glacial conditions.Ice Sheet advance into SW Dove Bugt

In Store Bælt, the orientation of glacial lineations (e.g. MSGL) suggest that ice flowed to the south along the west cost of Store Koldewey, marking the southwards expansion of the Storstrømmen ice stream (Fig. 9a & 9b). East of Dove Bugt, MSGL identified in Store Koldewey Trough are believed to have formed when the Storstrømmen ice stream acted as a “pure” ice stream (Bentley, 1987; Stokes and Clark, 1999) and overrode the underlying topography during the LGM (Fig. 9a ; Olsen et al., 2020). It was theorized that at a later phase, when the ice sheet began to thin, the ice stream became more influenced by the topography of deep troughs, draining northwards to Jøkelbugten and southwards to Dove Bugt (Olsen et al., 2020). Assuming these two phases occurred in the Storstrømmen ice stream development, it is quite possible that these glacial lineations in Store Bælt represent a period when a branch of the ice stream began conforming to topographical controls (e.g. Store Koldewey) and flowed towards the south. At this point the ice may have flowed to the southeast through Dove Bugt Trough, potentially also reaching the shelf break (Fig. 9a).

It is also possible that these MSGL formed during a glacial advance that followed the LGM (e.g. (Fig. 9b). Terrestrial moraines identified across the study area have been linked to different

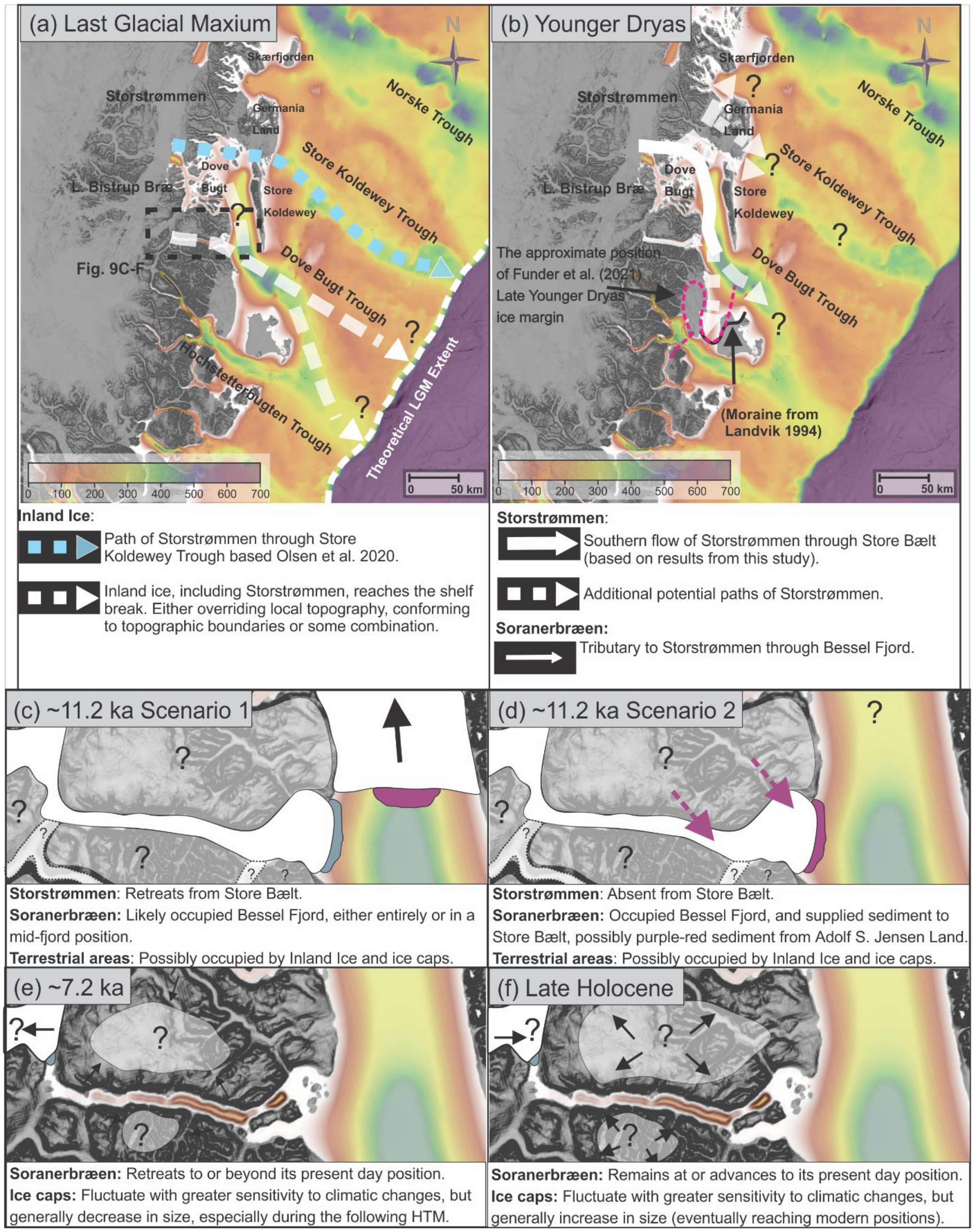

Figure 9. Maps showing ice sheet extent and advancement/retreat directions in SW Dove Bugt and Bessel Fjord (a) during the LGM, (b) during the Younger Dryas, (c & d) ~11.2 ka, (e) ~7.2 ka and (f) the Late Holocene. The black arrows in c-f represent the general direction of ice advancement/retreat. The size of ice caps in c-f are only indicative. Grey and purple-red colors in front of glaciers represent sediment input from over and under-flows. Purple dashed arrows represent the potential source of purple-red sediment found in Store Bælt. Background bathymetry displayed using IBCAO data (Jakobsson et al., 2020).

https://doi.org/10.5194/egusphere-2022-970
Preprint. Discussion started: 11 October 2022

glacial events (Fig. 10a), including the Nanok II Stadial, which is believed to have formed during the Younger Dryas (12.9–11.7 ka BP) (Vasskog et al., 2015). Between Hochstetter Forland and Shannon Ø a submerged moraine has been identified in Shannon Sound, which may indicate that at one point, possibly during the Younger Dryas, the ice stream travelled south rather than through Dove Bugt Trough (Hjort, 1981; Landvik, 1994). Larsen et al. (2016) placed the ice margin at the Shannon Sound moraine, as well as across Store Koldewey, Hochstetter Forland, and Shannon Ø giving it an age within late Allerød/early Younger Dryas. Later, Funder et al. (2021) excluded the moraines at Store Koldewey as part of the ice margin and placed the margin within late Younger Dryas (Fig. 9b). These ice margin interpretations are further supported by the proposed deglaciation date of Store Bælt at ~11.2 ka, which follows the Younger Dryas (see below).

5.2. Ice Sheet retreat through Store Bælt

The change from glacimarine and glacier front proximal mud (unit 1.1) in core HH17-1309 to glacimarine glacier front distal (unit 1.2) represent a “transition zone” marking the deglaciation in the region (Figs. 7 & 8e). The deglaciation has been dated to ~11.2 ka (Table 4).

This deglaciation age of 11.2 ka is attributed to a N-S bound branch of the NGIS (Fig. 9c) rather than a W-E flowing ice body from Bessel Fjord (e.g. Fig 9d) due to the presence of N-S oriented glacial lineations near the gravity core and a lack of morainal features that would provide evidence for an W-E bound GrIS or ice caps encroaching on Dove Bugt. Previously published dates constraining the timing of deglaciation in Dove Bugt have been restricted to terrestrial regions (Fig. 10b). Skov et al., (2020) produced deglaciation ages of ca. 12.7 ka at Store Koldewey and ca. 9.8 ka at Pusterdal with the application of cosmogenic nuclide dating on low to mid-elevation (100-460 m) bedrock. Further north, in eastern North Greenland, Larsen et al. (2020) found that ice in deep fjords retreated rapidly from the outer coast to the present ice margin between ~11 and 10 ka.

Radiocarbon dates obtained from lake sediments on Store Koldewey suggest that the earliest onset of warmth may have begun around 10 ka (Klug et al., 2009), therefore, the deglaciation of the area beginning just prior to this may further support these results. Additionally, Bennike & Weidick (2001) compiled previously published radiocarbon dates that represent the minimum date for deglaciation across Northeast Greenland. On the southern coast of Germania Land a minimum age of 9.5 ka BP has been presented (Bennike & Weidick, 2001), although earlier studies on Germania Land suggest that the ice front may have been east of the present day coastline until 19 ka BP and retracted to its current position by 7.5 ka BP (Landvik, 1994; Weidick et al., 1996). On Hochstetter Forland, Bennike & Weidick (2001) presented a minimum age of 11.2 ka, although a later study by Klug et al. (2016) presented a larger range of deglaciation ages for Hochstetter Foland and other nearby regions (Fig. 10b).

The radiocarbon date of ~11.2 ka from HH17-1309 largely matches findings on Store Koldewey and Hochstetter Forland (e.g. Bennike & Weidick, 2001; Skov et al., 2020). It is slightly earlier to those obtained by Larsen et al. (2020) on the outer coast and deep fjords in eastern North Greenland, which placed the deglaciation between 11 and 10 ka. Store Koldewey may have been partially deglaciated prior to the retreat of the NGIS through Store Bælt, where Hochstetter Forland may have been fully or partially glaciated.

https://doi.org/10.5194/egusphere-2022-970
Preprint. Discussion started: 11 October 2022

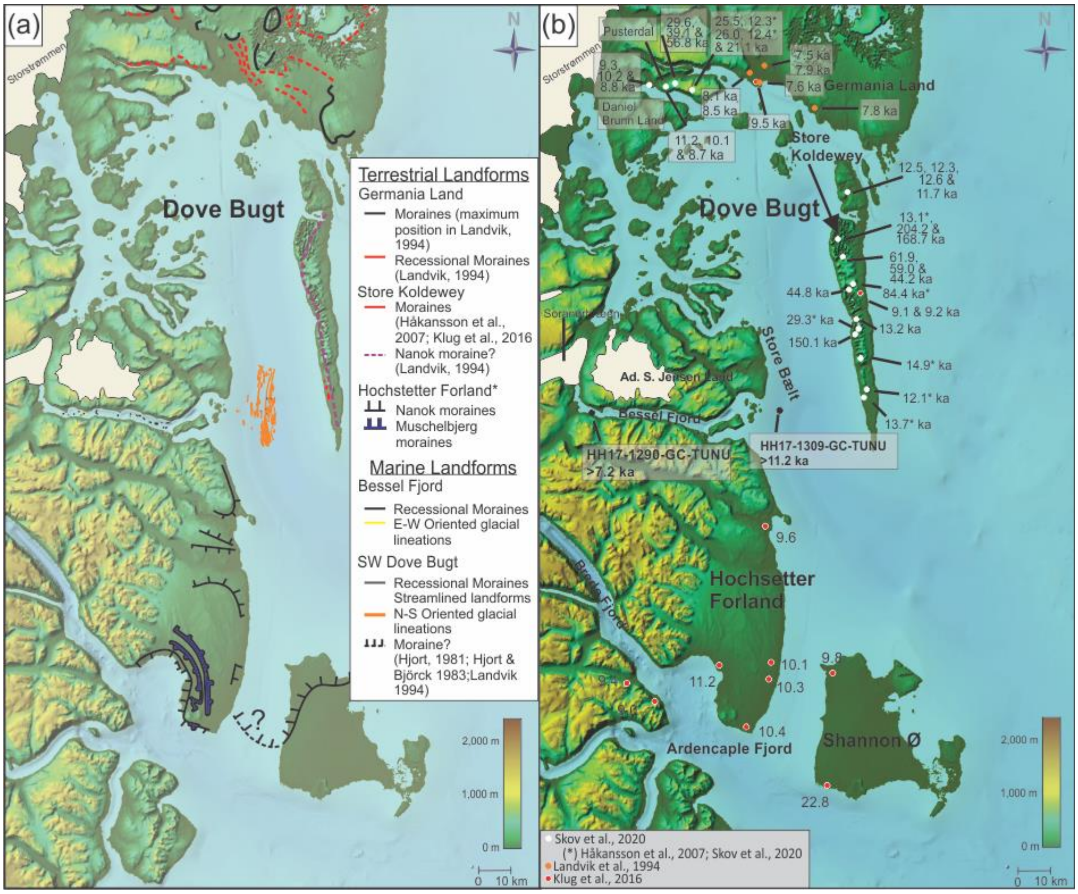

Figure 10. (a) Marine moraine ridges and glacial lineations from the current study together with previously mapped marine and terrestrial features. (b) Location of the current marine radiocarbon dates are indicated by filled black circles. Background displayed using IBCAO data (Jakobsson et al., 2020).

Although based on a limited data set, the lack of prominent morainal landforms in Store Bælt may also suggest a rapid retreat through the region. A small number of retreat moraines have been observed in an isolated region of the study area, but the most prominent geomorphic landforms are glacial lineations. Placing Store Bælt within the context of Dowdeswell et al. (2008)'s proposed model for ice streams in high latitudes, ice likely retreated through the area rapidly, although the presence of small moraines may suggest brief periods of stagnation. This is in accordance with findings by Larsen et al. (2020) that deep fjords and outer regions in eastern North Greenland were rapidly deglaciated between ~11 and 10 ka. However, additional data is required to confirm this.

5.3. Ice Sheet retreat through Bessel Fjord

The appearance of recessional moraines in Bessel Fjord suggests that the fjord underwent a stepwise deglaciation. The large moraine identified between Basin 3 and Basin 4 (M3; Fig. 7e) is believed to have formed during a major ice halt or readvance. Smaller moraines occasionally follow topographic boundaries, which may suggest that the retreat of ice in Bessel Fjord was

https://doi.org/10.5194/egusphere-2022-970
Preprint. Discussion started: 11 October 2022

also partly topographically controlled. Recessional moraines identied by Olsen et al (2020) east of Dove Bugt in Store Koldewey contain a similar height to those identified here (excluding M3), however moraines identified on the shelf appear more numerous and are wider, likely due to the lack of topographic confinment.

If the deglaciation of the fjord started immediately after the deglaciation of Store Belt, the radiocarbon date of ~11.2 ka from HH17-1309 represent a maximum age for the onset of the deglaciation of Bessel fjord. Gravity core HH17-1290, collected from the inner fjord region, consists of sediments that reflect an increasingly ice distal environment up core. One radiocarbon date from the core provides a minimum age of ~7.2 ka for the deglaciation of Soranerbræen and/or local ice caps from the inner fjord region (Table 4 & Fig. 9e). This date, however, is not from the base of the deglacial deposits and therefore represents a minimum age for the deglaciation of the inner fjord. This minimum age of 7.2 ka BP falls within a modelled ice sheet extent by Lecavalier et al. (2014) which placed the position of the ice sheet in the middle of Bessel Fjord at 9 ka BP and that the present-day ice margin is reached by 6 ka BP. The minimum age also agrees with the onset of HTM on Store Koldewey (~8.0 to 4.0 ka) (Wagner et al., 2008; Klug et al., 2009; Schmidt et al., 2011) and Hochstetter Forland (8.8 and 5.6 ka) (Björck & Persson, 1981; Björck et al., 1994), while findings from Melles Lake suggest that the onset of warmth may have occurred earlier, at ~ 10 ka (Klug et al., 2009). Thus, the GrIS retreated from the marine realm in early Holocene, slightly before or at the time of the HTM in this region (characterized by a mean July temperature 2-3°C higher than at present; Bennike et al., 2008).

From this we suggest that increased Northern Hemisphere summer insolation that peaked in the early Holocene was the main control for this part of the deglaciation during which the ice front receded from the coastline to the west of (onshore) Bessel fjord, a distance of ~60 km. Assuming that this occurred over a maximum period of ~4 ka (11.2 – 7.2 ka, however, likely over a shorter period, see discussion above), this corresponds to an average ice recession rate of ~15 m/yr. This rate is considered realistic as it is half (or less) than the rate estimated from the Nioghalvfjerdsfjorden further north (also part of the Storstrømmen ice stream) where a rate of ~30 – 40 m/yr was reported (Bennike & Björck, 2002).

5.4. Holocene glacier variability and sedimentary processes in Dove Bugt

Sedimentological evidence (e.g. rhythmically-laminated muds) from HH17-1309 suggests, that suspension settling from a glacial source(s) likely dominated southwestern Dove Bugt during the Holocene. The contribution of sediment from the NGIS seems unlikely, as Pusterdal became deglaciated by 9.5 ka BP (Skov et al., 2020) and Storstrømmen retreated to its modern day position by 7.5 ka BP (Weidick et al., 1994), therefore it very well may be from Soranerbræen, or perhaps more likely, local ice caps. It is possible that local ice caps and/or Soranerbræen advanced during short lived, cold reversals (i.e. ~11.4, 9.3, and 8.2 ka BP) (Rasmussen et al., 2007; Vasskog et al., 2015) or had a delayed response to warming, which may have contributed to the deposition of additional sediment in Store Bælt (see below for add conjecture concerning ice cap fluctuations).

During the later part of the HTM in the middle Holocene, a time period in which some glaciers are believed to have reached their minimum extent across Greenland, the NGIS is believed to have retreated beyond its current position between 6 to 1 ka BP, creating the Storstrømmen Sound (Weidick et al., 1994). Relating the core sedimentology to a linear age model developed from sedimentation rates (i.e. Table 4), laminations appear less frequently in core HH17-1309 during this period, yet they are not absent. Laminations are entirely absent in the Bessel Fjord core HH17-1290 during this period and remain absent through the colder Late Holocene. During the Little Ice Age Storstrømmen is believed to have expanded to its modern day position (Weidick et al., 1994).

Gravity core HH17-1289, collected to the north of an onshore glaciofluvial channel connected to a modern-day ice cap, transitions to complex assortment of sand layers just prior to 3,544 cal yr BP (Fig. 7). Sedimentological evidence suggests that these sand layers are largely the result of rapid, short lived depositional events (i.e. turbidity currents) interpreted to be related to the growth of a delta slightly south of the core site, from glacifluvial sediment input from a nearby outlet glacier.

Exposure dates in the region show that the HTM ended between 5.6-4 yr BP in this area (Briner et al., 2016), coinciding with the onset of turbidites in core HH17-1289. Therefore, it is possible that this shift to sand dominated sedimentation within this core was controlled by climatically driven processes. This onset is here suggested to result from higher sediment input through the channel as local ice caps expanded outwards following the HTM, possibly in response to this climate cooling (Fig. 9f). There is however an absence of sedimentological data in the Inner Fjord region to suggest that Soranerbræen readvanced beyond its modern-day position during the Late Holocene (Fig. 7).

5.5. Sea ice cover during the Holocene

Lake studies suggest that the HTM occurred between ~8 and 4 ka on Store Koldewey (or as early as ~10 ka) (Wagner et al., 2008; Klug et al., 2009; Schmidt et al., 2011; Briner et al., 2016) and between 8.8 and 5.6 ka on Hochstetter Forland (Björck & Persson, 1981; Björck et al., 1994). Corresponding to the HTM in Bessel fjord, one would expect to see less sea-ice and higher marine productivity. However, this is not reflected in the Ca/Fe ratios. Instead, Ca/Fe ratios are decreasing between 8.5 ka to 1 ka and only increase slightly thereafter, without any peak corresponding to an increased marine productivity during the HTM.

The decrease in values up core in Bessel Fjord may represent a decrease in palaeo-productivity and an increase in sea cover over time. If this is the case, the HTM is not reflected in the Ca/Fe ratios, which either implies that Bessel Fjord was gradually covered in sea ice for a larger part of the year throughout the Holocene (~10 months a year at present) or that Ca/Fe ratios do not reflect sea ice conditions within the fjord, or the lack thereof. Further studies are needed to clarify this. Minor fluctuations in Ca/Fe ratios near the base of HH17-1290, and peak (or the absence of peaks) identified throughout HH17-1289 reflect turbidite deposition, as Ca/Fe ratios can be effective in distinguishing between turbidites and pelagites (Rothwell et al., 2006).

6. Conclusion

In summary:

- Glacial lineations (MSGLs) identified in SW Dove Bugt suggest fast-flowing ice, interpreted to be from the NGIS, developed during the LGM or at a later (deglacial) ice readvance.
- The timing of this deglaciation (>11.2 ka) from this study is later than recent deglaciation dates from the island of Store Koldewey (Skov et al., 2020) but are in conformity or

https://doi.org/10.5194/egusphere-2022-970
Preprint. Discussion started: 11 October 2022

earlier then deglaciation dates on Hochstetter Forland slightly south of the study area (Klug et al., 2016).

- Deglaciation of the Bessel Fjord is interpreted to have started immediately after the deglaciation of Dove Bugt, i.e., < 11.2 ka (in the Preboreal).
- Moraines in Bessel Fjord suggests that the fjord underwent multiple halts/or readvances upon deglaciation. Thus, the bathymetry of Bessel Fjord (to the west of Dove Bugt) indicates that the glacial dynamics of the fjord were more dynamic than onshore evidence suggests.
- The radiocarbon date of 7.2 ka BP obtained in an inner fjord core is interpreted as a minimum age at which Soranerbræen retreated to or beyond its present-day onshore position west of the fjord.
- Ice recession in Bessel Fjord occurred at a minimum average rate of ~15 m/yr.
- The GrIS retreated from the marine realm in the early Holocene, around the time of the Holocene Thermal Maximum in this region. From this we suggest that increased Northern Hemisphere summer insolation that peaked in the early Holocene was the main control for this part of the deglaciation (the mean July temperature then was according to Bennike et al. (2008) at least 2-3 °C higher than at present).
- A low sedimentation rate of 13.55 cm/ka after 7.2 ka BP, and the presence of only massive mud, suggests that Soranerbræen did not expand back into Bessel Fjord for the remainder of the Holocene.
- The transition of mud to muddy sand at 4 ka BP in a mid-fjord core may provide evidence for ice cap growth. Thus, ice caps in Bessel Fjord were fluctuating with greater sensitivity to climatic conditions than the NE sector of the GrIS during the cooling phase that followed the HTM.

Data availability: The bathymetry and core data from UiT The Arctic University of Norway will be available upon reasonable request at UiT's open research data repository: https://dataverse.no/dataverse/uit.

Author contributions: Jan Sverre Laberg and Tom Arne Rydningen designed this study and collected the new data during the 2017 TUNU VII cruise. The bathymetrical and lithological data were interpreted by Kevin Zoller in collaboration with Jan Sverre Laberg and Tom Arne Rydningen. Kevin Zoller prepared the manuscript with contributions from all co-authors.

Competing interests: The authors declare that they have no conflict of interest.

Acknowledgement: We would like to thank the participants of the 2017 TUNU cruise to Greenland for making this project possible. A special thanks to the captain and crew of the RV *Helmer Hanssen* for their involvement in the cruise and assistance in collecting the data. A thanks also goes out to the lab staff at UiT, Trine Dahl, Karina Monsen and Ingvild Hald, who assisted with processing sediment core samples for this project. We would also like to thank Gesine Mollenhauer and the lab staff at the Alfred Wegener Institut for providing us with radiocarbon dated material using their MICADAS. Funding for this work was provided by UiT The Arctic University of Norway.

https://doi.org/10.5194/egusphere-2022-970
Preprint. Discussion started: 11 October 2022

References

Arndt, J. E.: Marine geomorphological record of Ice Sheet development in East Greenland since the Last Glacial Maximum, J. Quat. Sci., 33, 853–864, https://doi.org/10.1002/jqs.3065, 2018.

Arndt, J. E., Jokat, W., Dorschel, B., Myklebust, R., Dowdeswell, J. A., and Evans, J.: A new bathymetry of the Northeast Greenland continental shelf: Constraints on glacial and other processes, AGU Publ. Geochemistry Geophys. Geosystems, 16, 267–300, https://doi.org/10.1002/2014GC005684.Key, 2015.

Arndt, J. E., Jokat, W., and Dorschel, B.: The last glaciation and deglaciation of the Northeast Greenland continental shelf revealed by hydro-acoustic data, Quat. Sci. Rev., 160, 45–56, 2017.

Barnes, P. M., Pickrill, R. A., and Bostock, H. C.: Thompson and Bradshaw sounds, Fiordland, New Zealand: a relict, mid-latitude, temperatue glacier system, in: Atlas of Submarine Glacial Landforms: Modern, Quaternary and Ancient, edited by: Dowdeswell, J. A., Canals, M., Jakobsson, M., Todd, B. J., Dowdeswell, E. K., and Hogan, K. A., The Geological Society of London, 45–46, 2016.

Bennike, O. and Björck, S.: Chronology of the last recession of the Greenland Ice Sheet, J. Quat. Sci., 17, 211–219, https://doi.org/10.1002/jqs.670, 2002.

Bennike, O. and Weidick, A.: Late Quaternary history around Nioghalvfjerdsfjorden and Jøokelbugten, North-East Greenland, Boreas, 30, 205–227, https://doi.org/10.1111/j.1502-3885.2001.tb01223.x, 2001.

Bennike, O., Sørensen, M., Fredskild, B., Jacobsen, B. H., BöCher, J., Amsinck, S. L., Jeppesen, E., Andreasen, C., Christiansen, H. H., and Humlum, O.: Late Quaternary Environmental and Cultural Changes in the Wollaston Forland Region, Northeast Greenland, Adv. Ecol. Res., 40, 45–79, https://doi.org/10.1016/S0065-2504(07)00003-7, 2008.

Bentley, C. R.: Antarctic ice streams: a review, Geophys. Res., 92(6), 8843–8858, 1987.

Björck, S. and Persson, T.: Late Weichselian and Flandrian biostratigraphy and chronology from hochstetter forland, northeast Greenland, Medd. Om. Grønl. Geosci., 5, 1–19, 1981.

Björck, S., Wohlfarth, B., Bennike, O., Hjort, C., and Persson, T.: Revision of the early Holocene lake sediment based chronology and event stratigraphy on Hochstetter Forland, NE Greenland, Boreas, 23, 513–523, https://doi.org/10.1111/j.1502-3885.1994.tb00619.x, 1994.

Boulton, G. S. and Deynoux, M.: Sedimentation in glacial environments and the identification of tills and tillites in ancient sedimentary sequences, Precambrian Res., 15, 397–422, https://doi.org/10.1016/0301-9268(81)90059-0, 1981.

Boulton, G. S., Hagdorn, M., and Hulton, N. R. J.: Streaming flow in an ice sheet through a glacial cycle, Ann. Glaciol., 36, 117–128, https://doi.org/10.3189/172756403781816293, 2003.

Briner, J. P., McKay, N. P., Axford, Y., Bennike, O., Bradley, R. S., de Vernal, A., Fisher, D., Francus, P., Fréchette, B., Gajewski, K., Jennings, A., Kaufman, D. S., Miller, G., Rouston, C., and Wagner, B.: Holocene climate change in Arctic Canada and Greenland, Quat. Sci. Rev., 147, 340–364, https://doi.org/10.1016/j.quascirev.2016.02.010, 2016.

Cartigny, M. J. B., Postma, G., Berg, J. H., and Mastbergen, D. R.: A comparative study of sediment waves and cyclic steps based on geometries, internal structures and numerical modeling, Mar. Geol., 280, 40–56, 2011.

Christiansen, J. S.: The TUNU-Programme : Euro-Arctic Marine Fishes — Diversity and Adaptation, in: Adaptation and Evolution in Marine Environments, vol. 1, 35–50, https://doi.org/10.1007/978-3-642-27352-0, 2012.

Clark, C. D.: Mega-scale lineations and cross-cutting ice-flow landforms, Earth Surf. Process. Landforms, 18, 1–29, 1993.

Clark, C. D. and Stokes, C. R.: Palaeo-ice stream landsystem, in: Glacial Landscapes, edited by: Evans, D. J. A., Edward Arnold, London, 204–227, 2003.

Clark, C. D., Tulaczyk, S. M., Stokes, C. R., and Canals, M.: A groove-ploughing theory for the production of mega-scale glacial lineations, and implications for ice-stream mechanics, J. Glaciol., 49, 240–256, https://doi.org/10.3189/172756503781830719, 2003.

Cohen, J., Screen, J. A., Furtado, J. C., Barlow, M., Whittleston, D., Coumou, D., Francis, J., Dethloff, K., Entekhabi, D., Overland, J., and Jones, J.: Recent Arctic amplification and extreme mid-latitude weather, Nat. Publ. Gr., 7, 627–637, https://doi.org/10.1038/ngeo2234, 2014.

Cowan, E. A., Seramur, K. C., Cai, J., and Powell, R. D.: Cyclic sedimentation produced by fluctuations in meltwater discharge, tides and marine productivity in an Alaskan fjord, Sedimentology, 46, 1109–1126, https://doi.org/10.1046/j.1365-3091.1999.00267.x, 1999.

Cremer, H., Bennike, O., and Wagner, B.: Lake sediment evidence for the last deglaciation of eastern Greenland, Quat. Sci. Rev., 27, 312–319, https://doi.org/10.1016/j.quascirev.2007.09.004, 2008.

Dowdeswell, J. A., Ottesen, D., Evans, J., Cofaigh, C. Ó., and Anderson, J. B.: Submarine glacial landforms and rates of ice-stream collapse, Geology, 36, 819–822, https://doi.org/10.1130/G24808A.1, 2008.

Dowdeswell, J. A., Canals, M., Jakobsson, M., Todd, B. J., Dowdeswell, E. K., and Hogan, K. A.: The variety and distribution of submarine glacial landforms and implications for ice-sheet reconstruction, Geol. Soc. Mem., 46, 519–552, https://doi.org/10.1144/M46.183, 2016.

Evans, J., Ó Cofaigh, C., Dowdeswell, J. A., and Wadhams, P.: Marine geophysical evidence for former expansion and flow of the Greenland Ice Sheet across the north-east Greenland continental shelf, J. Quat. Sci., 24, 279–293, 2009.

Eyles, N., Eyles, C. H., and Niall, An. D.: Lithofacies types and vertical profile models; an alternative approach to the description and environmental interpretation of glacial diamict and diamictite sequences, Sedimentology, 30, 393–410, 1983.

Folk, R. L.: The Distinction between Grain Size and Mineral Composition in Sedimentary-Rock Nomenclature, J. Geol., 62, 344–359, 1954.

Folk, R. L. and Ward, W.: Brazos river bar, a study in the significance of grain size parameters., J. Sediment. Petrol., 27, 34–59, 1957.

Forwick, M. and Vorren, T. O.: Deglaciation history and post-glacial mass movements in Balsfjord, northern Norway, Polar Res., 21(2), 259–266, 1998.

Forwick, M. and Vorren, T. O.: Late Weichselian and Holocene sedimentary environments and ice rafting, Palaeogeogr. Palaeoclimatol. Palaeoecol., 280, 258–274, 2009.

Forwick, M., Vorren, T. O., Hald, M., Korsun, S., Roh, Y., Vogt, C., and Yoo, K. C.: Spatial and temporal influence of glaciers and rivers on the sedimentary environment in Sassenfjorden and

https://doi.org/10.5194/egusphere-2022-970
Preprint. Discussion started: 11 October 2022

Tempelfjorden, Spitsbergen, Geol. Soc. London, Spec. Publ., 344, 163–193, https://doi.org/10.1144/SP344.13, 2010.

Funder, S.: 14C-dating of samples collected during the 1979 expedition to North Greenland., 9–13 pp., 1982.

Funder, S., Kjeldsen, K. K., Kjær, H. K., and Ó Cofaigh, C.: The Greenland Ice Sheet During the Past 300,000 Years: A Review, Dev. Quat. Sci., 15, 699–713, https://doi.org/10.1016/B978-0-444-53447-7.00050-7, 2011.

Funder, S., Sørensen, A. H. L., Larsen, N. K., Bjørk, A. A., Briner, J. P., Olsen, J., Schomacker, A., Levy, L. B., and Kjær, K. H.: Younger Dryas ice margin retreat in Greenland : new evidence from southwestern Greenland, 587–601, 2021.

Håkansson, S.: University of Lund Radiocarbon Dates VI, Radiocarbon, 15, 493–513, 1973.

Henriksen, N. and Higgins, A. K.: Descriptive text to the Geological map of Greenland, 1:500 000, Lambert Land, Sheet 9, Series 4., Geological Survey of Denmark and Greenland Map Series, 1–32 pp., 2009.

Higgins, A. K.: North Greenland Glaeier Velocities and Calf Ice Production, Polarforschung, 60, 1–23, 1991.

Hill, P. R.: Changes in submarine channel morphology and strata development from repeat multibeam surveys in the Fraser River delta, western Canada, in: Sediments, Morphology and Sedimentary Processes on Continental Shelves, edited by: Li, M. Z., Sherwood, C. R., and Hill, P. R., Blackwell Science, International Association of Sedimentologists, 47–70, 2012.

Hjort, C.: Glaciation in northern East Greenland during the Late Weichselian and Early Flandrian, Boreas, 8, 281–296, https://doi.org/10.1111/j.1502-3885.1979.tb00812.x, 1979.

Hjort, C.: A glacial chronology for northern East Greenland, Boreas, 10, 259–274, 1981.

Hjort, C. and Björck, S.: A re-evaluated glacial chronology for Northern East Greenland, Gff, 105, 235–243, https://doi.org/10.1080/11035898309452590, 1983.

Hogan, K. A., Dowdeswell, J. A., Noormets, R., Evans, J., and Ó Cofaigh, C.: Evidence for full-glacial flow and retreat of the Late Weichselian Ice Sheet from the waters around Kong Karls Land, eastern Svalbard, Quat. Sci. Rev., 29, 3563–3582, https://doi.org/10.1016/j.quascirev.2010.05.026, 2010.

Hogan, K. A., Ó Cofaigh, C., Jennings, A. E., Dowdeswell, J. A., and Hiemstra, J. F.: Deglaciation of a major palaeo-ice stream in Disko Trough, West Greenland, Quat. Sci. Rev., 147, 5–26, 2016.

Jakobsson, M., Mayer, L. A., Bringensparr, C., Castro, C. F., Mohammad, R., Johnson, P., Ketter, T., Accettella, D., Amblas, D., An, L., Arndt, J. E., Canals, M., Casamor, J. L., Chauché, N., Coakley, B., Danielson, S., Demarte, M., Dickson, M. L., Dorschel, B., Dowdeswell, J. A., Dreutter, S., Fremand, A. C., Gallant, D., Hall, J. K., Hehemann, L., Hodnesdal, H., Hong, J., Ivaldi, R., Kane, E., Klaucke, I., Krawczyk, D. W., Kristoffersen, Y., Kuipers, B. R., Millan, R., Masetti, G., Morlighem, M., Noormets, R., Prescott, M. M., Rebesco, M., Rignot, E., Semiletov, I., Tate, A. J., Travaglini, P., Velicogna, I., Weatherall, P., Weinrebe, W., Willis, J. K., Wood, M., Zarayskaya, Y., Zhang, T., Zimmermann, M., and Zinglersen, K. B.: The International Bathymetric Chart of the Arctic Ocean Version 4.0, Sci. Data, 7, 1–14, https://doi.org/10.1038/s41597-020-0520-9, 2020.

https://doi.org/10.5194/egusphere-2022-970
Preprint. Discussion started: 11 October 2022

Kempf, P., Forwick, M., Laberg, J. S., and Vorren, T. O.: Late Weichselian and Holocene sedimentary palaeoenvironment and glacial activity in the high-arctic van Keulenfjorden, Spitsbergen, The Holocene, 23 (11), 1607–1618, https://doi.org/10.1177/0959683613499055, 2013.

Khan, S. A., Kjær, K. H., Bevis, M., Bamber, J. L., Wahr, J., Kjeldsen, K. K., Bjørk, A. A., Korsgaard, N. J., Stearns, L. A., Van Den Broeke, M. R., Liu, L., Larsen, N. K., and Muresan, I. S.: Sustained mass loss of the northeast Greenland ice sheet triggered by regional warming, Nat. Clim. Chang., 4, 292–299, https://doi.org/10.1038/nclimate2161, 2014.

King, E. C., Hindmarsh, R. C. A., and Stokes, C. R.: Formation of mega-scale glacial lineations observed beneath a West Antarctic ice stream, Nat. Geosci., 2, 585–588, https://doi.org/10.1038/ngeo581, 2009.

King, M. D., Howat, I. M., Candela, S. G., Noh, M. J., Jeong, S., Noël, B. P. Y., van den Broeke, M. R., Wouters, B., and Negrete, A.: Dynamic ice loss from the Greenland Ice Sheet driven by sustained glacier retreat, Commun. Earth Environ., 1, 1–7, https://doi.org/10.1038/s43247-020-0001-2, 2020.

Klages, J. P., Kuhn, G., Hillenbrand, C.-D., Graham, A. G. C., Smith, J. A., Larter, R. D., and Gohl, K.: First geomorphological record and glacial history of an inter-ice stream ridge on the West Antarctic continental shelf, Quat. Sci. Rev., 61, 47–61, 2013.

Klages, J. P., Kuhn, G., Graham, A. G. C., Hillenbrand, C.-D., Smith, J. A., Nitsche, F. O., Larter, R. D., and Gohl, K.: Palaeo-ice stream pathways and retreat style in the easternmost Amundsen Sea Embayment, West Antarctica, revealed by combined multibeam bathymetric and seismic data, Geomorphology, 245, 207–222, 2015.

Klug, M., Schmidt, S., Melles, M., Wagner, B., Bennike, O., and Heiri, O.: Lake sediments from Store Koldewey, Northeast Greenland, as archive of Late Pleistocene and Holocene climatic and environmental changes, Boreas, 38, 59–71, https://doi.org/10.1111/j.1502-3885.2008.00038.x, 2009a.

Klug, M., Bennike, O., and Wagner, B.: Repeated short-term bioproductivity changes in a coastal lake on Store Koldewey, northeast Greenland: An indicator of varying sea-ice coverage?, Holocene, 19, 653–663, https://doi.org/10.1177/0959683609104040, 2009b.

Klug, M., Bennike, O., and Wagner, B.: Late Pleistocene to early Holocene environmental changes on Store Koldewey, coastal north-east Greenland, Polar Res., 35, https://doi.org/10.3402/polar.v35.21912, 2016.

Laberg, J. S., Forwick, M., and Husum, K.: New geophysical evidence for a revised maximum position of part of the NE sector of the Greenland ice sheet during the last glacial maximum, Arktos, 3, https://doi.org/10.1007/s41063-017-0029-4, 2017.

Lambeck, K., Rouby, H., Purcell, A., Sun, Y., and Sambridge, M.: Sea level and global ice volumes from the Last Glacial Maximum to the Holocene, Proc. Natl. Acad. Sci., 111, 15296–15303, https://doi.org/10.1073/pnas.1411762111, 2014.

Landvik, J. Y.: The last glaciation of Germania Land and adjacent areas, northeast Greenland, J. Quat. Sci., 9, 81–92, https://doi.org/10.1002/jqs.3390090108, 1994.

Larsen, N. K., Funder, S., Linge, H., Möller, P., Schomacker, A., Fabel, D., Xu, S., and Kjær, K. H.: A Younger Dryas re-advance of local glaciers in north Greenland, Quat. Sci. Rev., 147, 47–58, https://doi.org/10.1016/j.quascirev.2015.10.036, 2016.

https://doi.org/10.5194/egusphere-2022-970
Preprint. Discussion started: 11 October 2022

Larsen, N. K., Levy, L. B., Carlson, A. E., Buizert, C., Olsen, J., Strunk, A., Bjørk, A. A., and Skov, D. S.: Instability of the Northeast Greenland Ice Stream over the last 45,000 years, Nat. Commun., 9, 3–10, https://doi.org/10.1038/s41467-018-04312-7, 2018.

Larsen, N. K., Søndergaard, A. S., Levy, L. B., Olsen, J., Strunk, A., Bjørk, A. A., and Skov, D.: Contrasting modes of deglaciation between fjords and inter-fjord areas in eastern North Greenland, Boreas, 49, 905–919, https://doi.org/10.1111/bor.12475, 2020.

Lyså, A. and Vorren, T. O.: Seismic facies and architecture of ice-contact submarine fans in high-relief fjords, Troms, Northern Norway, Boreas, 26, 309–328, 1997.

Mouginot, J., Rignot, E., Scheuchl, B., Fenty, I., Khazendar, A., Morlighem, M., Buzzi, A., and Paden, J.: Fast retreat of Zachariae Isstrom, Northeast Greenland, Science (80-.)., 350, 1357–1361, 2015.

Mouginot, J., Bjørk, A. A., Millan, R., Scheuchl, B., and Rignot, E.: Insights on the Surge Behavior of Storstrømmen and L. Bistrup Bræ, Northeast Greenland, Over the Last Century, Geophys. Res. Lett., 45, 11,197-11,205, https://doi.org/10.1029/2018GL079052, 2018.

Ó Cofaigh, C.: Flow Dynamics and till genesis associated with a marin-based Antarctic palaeo-ice stream, Quat. Sci. Rev., 24, 709–740, 2005.

Ó Cofaigh, C., Dowdeswell, J. A., Jennings, A. E., Hogan, K. A., Kilfeather, A., Hiemstra, J. F., Noormets, R., Evans, J., McCarthy, D. J., Andrews, J. T., Lloyd, J. M., and Moros, M.: An extensive and dynamic ice sheet on the west greenland shelf during the last glacial cycle, Geology, 41, 219–222, https://doi.org/10.1130/G33759.1, 2013.

Olsen, I. L., Forwick, M., Laberg, J. S., and Rydningen, T. A.: Last Glacial ice-sheet dynamics offshore NE Greenland – a case study from Store Koldewey Trough, The Cryosphere Discussions, 2020.

Olsen, I. L., Laberg, J. S., Forwick, M., Rydningen, T. A., and Husum, K.: Late Weichselian and Holocene behavior of the Greenland Ice Sheet in the Kejser Franz Josef Fjord system, NE Greenland, Quat. Sci. Rev., 2022.

Ottesen, D., Dowdeswell, J. A., Benn, D. I., Kristensen, L., Christiansen, H. H., Christensen, O., Hansen, L., Lebesbye, E., Forwick, M., and Vorren, T. O.: Submarine landforms characteristic of glacier surges in two spitsbergen fjords, Quat. Sci. Rev., 27, 1583–1599, 2008.

Passchier, S.: Soft-Sediment Deformation Features in Core from CRP-2 / 2A , Victoria Land Basin, Antarctica, Terra Antarct., 7(3), 401–412, 2000.

Rahmstorf, S., Box, J. E., Feulner, G., Mann, M. E., Robinson, A., Rutherford, S., and Schaffernicht, E. J.: Exceptional twentieth-century slowdown in Atlantic Ocean overturning circulation, Nat. Clim. Chang., 5, 475–480, https://doi.org/10.1038/nclimate2554, 2015.

Rasmussen, S. O., Vinther, B. M., Clausen, H. B., and Andersen, K. K.: Early Holocene climate oscillations recorded in three Greenland ice cores, Quat. Sci. Rev., 26, 1907–1914, 2007.

Reeh, N., Bøggild, C. E., and Oerter, H.: Surge of Storstrømmen, a large outlet glacier from the Inland Ice of North-East Greenland, Rapp. Grønands Geol. Unders., 162, 201–209, 1994.

Reimer, P. J., Bard, E., Bayliss, A., Beck, J. W., Blackwell, P. G., Bronk Ramsey, C., Buck, C. E., Cheng, H., Edwards, R. L., Friedrich, M., Grootes, P. M., Guilderson, T. P., Haflidason, H., Hajdas, I., Hatté, C., Heaton, T. J., Hoffmann, D. L., Hogg, A. G., Hughen, K. A., Kaiser, K. F., Kromer, B., Manning, S. W., Niu, M., Reimer, R. W., Richards, D. A., Scott, E. M., Southon, J.

https://doi.org/10.5194/egusphere-2022-970
Preprint. Discussion started: 11 October 2022

R., Staff, R. A., Turney, C. S. M., and van der Plicht, J.: Intcal13 and Marine13 Radiocarbon Age Calibration Curves 0–50,000 Years Cal Bp, Radiocarbon, 55, 1869–1887, 2013.

Rothwell, R. G., Hoogakker, B., Thomson, J., Croudace, I. W., and Frenz, M.: Turbidite emplacement on the southern Balearic Abyssal Plain (western Mediterranean Sea) during Marine Isotope Stages 1-3: An application of ITRAX XRF scanning of sediment cores to lithostratigraphic analysis, Geol. Soc. Spec. Publ., 267, 79–98, https://doi.org/10.1144/GSL.SP.2006.267.01.06, 2006.

Rydningen, T. A., Vorren, T. O., Laberg, J. S., and Kolstad, V.: The marine-based NW Fennoscandian ice sheet: Glacial and deglacial dynamics as reconstructed from submarine landforms, Quat. Sci. Rev., 68, 126–141, https://doi.org/10.1016/j.quascirev.2013.02.013, 2013.

Schmidt, S., Wagner, B., Heiri, O., Klug, M., Bennike, O., and Melles, M.: Chironomids as indicators of the Holocene climatic and environmental history of two lakes in Northeast Greenland, Boreas, 40, 116–130, https://doi.org/10.1111/j.1502-3885.2010.00173.x, 2011.

Schoof, C. G. and Clarke, G. K. C.: A model for spiral flows in basal ice and the formation of subglacial flutes based on a Reiner-Rivlin rheology for glacial ice, J. Geophys. Res. Solid Earth, 113, 1–12, https://doi.org/10.1029/2007JB004957, 2008.

Shaw, J., Pugin, A., and Young, R. R.: A meltwater origin for Antarctic shelf bedforms with special attention to megalineations, Geomorphology, 102, 364–375, https://doi.org/10.1016/j.geomorph.2008.04.005, 2008.

Shreve, R. L.: Esker characteristics in terms of glacier physics, Katahdin esker system, Maine., Geol. Soc. Am. Bull., 96, 639–646, https://doi.org/10.1130/0016-7606(1985)96<639:ECITOG>2.0.CO;2, 1985.

Skov, D. S., Andersen, J. L., Olsen, J., Jacobsen, B. H., Knudsen, M. F., Jansen, J. D., Larsen, N. K., and Egholm, D. L.: Constraints from cosmogenic nuclides on the glaciation and erosion history of Dove Bugt , northeast Greenland, GSA Bull., 1–13, 2020.

Stacey, C. D. and Hill, P. R.: Cyclic steps on a glacifluvial delta, Howe Sound, British Columbia, in: Atlas of Submarine Glacial Landforms: Modern, Quaternary and Ancient, edited by: Dowdeswell, J. A., Canals, M., Jakobsson, M., Todd, B. J., Dowdeswell, E. K. & Hogan, K. A., Geological Society of London, 93–94, 2016.

Stocker, T. F., Qin, D., Plattner, G.-K., Tignor, M. M. B., Allen, S. K., Boschung, J., Nauels, A., Xia, Y., Bex, V., and Midgley, P. M.: Climate Change 2013: The Physical Science Basis. Contribution of Working Group I to the Fifth Assessment Report of the Intergovernmental Panel on Climate Change, Cambridge, 2013.

Stokes, C. R. and Clark, C. D.: Geomorphological criteria for identifying Pleistocene ice streams, Ann. Glaciol., 28, 67–74, https://doi.org/10.3189/172756499781821625, 1999.

Stokes, C. R. and Clark, C. D.: Palaeo-ice streams, Quat. Sci. Rev., 20, 1437–1457, 2001.

Storrar, R. D., Stokes, C. R., and Evans, D. J. A.: Morphometry and pattern of a large sample (>20,000) of Canadian eskers and implications for subglacial drainage beneath ice sheets, Quat. Sci. Rev., 105, 1–25, https://doi.org/10.1016/j.quascirev.2014.09.013, 2014.

Stuiver, M. and Reimer, P. J.: Extended 14C data base and revised calib 3.0 14C age calibration program, Radiocarbon, 35, 215–230, 1993.

Vasskog, K., Langebroek, P. M., Andrews, J. T., Nilsen, J. E. Ø., and Nesje, A.: The Greenland

https://doi.org/10.5194/egusphere-2022-970
Preprint. Discussion started: 11 October 2022

Ice Sheet during the last glacial cycle: Current ice loss and contribution to sea-level rise from a palaeoclimatic perspective, Earth-Science Rev., 150, 45–67, https://doi.org/10.1016/j.earscirev.2015.07.006, 2015.

Wagner, B., Bennike, O., Bos, J. A. A., Cremer, H., Lotter, A. F., and Melles, M.: A multidisciplinary study of Holocene sediment records from Hjort Sø on Store Koldewey, Northeast Greenland, J. Paleolimnol., 39, 381–398, https://doi.org/10.1007/s10933-007-9120-3, 2008.

Weber, M. E., Niessen, F., Kuhn, G., and Wiedicke, M.: Calibration and application of marine sedimentary physical properties using a mult-sensor core logger, Mar. Geol., 136, 151–172, 1997.

Weidick, A., Andreasen, C., Oerter, H., and Reeh, N.: Neoglacial glacier changes around Storstrommen, north-east Greenland, Polarforschung, 64, 95–108, 1994.

Weidick, B. A., Andreasen-, C., Oerter, H., and Reeh, N.: Neoglacial Glacier Changes around Storstrommen, North-East Greenland, Polarforschung, 64, 95–108, 1996.

Winkelmann, D., Jokat, W., Jensen, L., and Schenke, H. W.: Submarine end moraines on the continental shelf off NE Greenland - Implications for Lateglacial dynamics, Quat. Sci. Rev., 29, 1069–1077, https://doi.org/10.1016/j.quascirev.2010.02.002, 2010.